

# The Borexino Neutrino Experiment

Borexino is a neutrino detector located deep underground in central Italy, under a thickness of rock equivalent to 3800 meters of water. It is expected to begin operations in Fall 2006, complementing the similarly designed but already operational KamLAND neutrino detector in Japan and the Čerenkov light detecting Sudbury Neutrino Observatory in Canada. Both of those detectors are targeted at higher-energy neutrinos. Borexino should be the first detector capable of observing sub-MeV solar neutrinos in real time. Indeed, its principal goal is to measure the  ${}^7\text{Be}$  neutrino flux to high accuracy. The possibility to measure the rates of the slightly higher-energy *pep* and CNO-cycle neutrinos is also foreseen. The expected operational lifetime of the experiment is ten years, which will give it a reasonable chance to observe neutrinos from a supernova in our galaxy or nearby. Measurements of neutrinos from other sources (geoneutrinos, reactor neutrinos) may also be feasible.

The name of the detector comes from “Borex,” since the fluid at the heart of the detector was originally planned to be trimethylborate-based [36], and “-ino,” the Italian suffix meaning “little,” as it was originally intended to be a prototype of a still-larger detector. Both parts of the name are now inaccurate, but it remains unchanged largely because of the well-known physics phenomenon of inertia. Various capitalizations are seen in the literature.

The principal reaction by which Borexino will detect neutrinos is elastic  $\nu e$  scattering. The neutrino is not seen directly, but it imparts some of its kinetic energy to an electron. As the electron travels, it is slowed down by ionizing interactions with the surrounding fluid medium. The 2200 photomultiplier tubes in Borexino will mainly observe light emitted by molecules of the target mass that were electronically excited by the ionizing processes. The target mass is referred to as a “scintillator,” and so Borexino is a scintillation detector.

Energy loss of a traveling charged particle also occurs via Čerenkov radiation. However, the number of Čerenkov photons detected will be at most a few percent of the total. Unlike Čerenkov light, scintillation light produced by excited molecules returning to their ground state is emitted isotropically. It will therefore not be possible to determine, even approximately, the initial direction of a neutrino that caused electron scattering in the detector.

In this chapter we discuss the radioactive backgrounds likely to be present in the Borexino detector (many of which have already been observed in its prototype Counting Test Facility) and the expected sensitivities of Borexino to neutrinos produced by various sources. A summary table is provided on the following page for quick reference.

## 2.1 Design parameters

Any radioactive decay inside the detector has some probability of being mistaken for a neutrino interaction. Many naturally occurring radioactive isotopes, in their decays, release energies in the sub-MeV range which is most important for the detector. Borexino is therefore designed around the principle of graded shielding, in which the central portion of the detector is the least contaminated. A detailed discussion of the detector scintillator and hardware can be found in Chapter 3. The following paragraphs, in tandem with Figure 3.1, should suffice to give a basic idea of the experimental design.

| Signal   | Source           | Expected events/day in FV |                      | References                   |
|--|------------------|---------------------------|----------------------|------------------------------|
|  |                  | 250–800 keV               | 0.8–1.3 MeV          |                              |
| <i>Internal backgrounds</i> (Individual isotopes are each also described in §2.2.2–2.2.3.) |                  |                           |                      |                              |
| $\mu^\pm, n$   | Cosmic rays      | $\sim 285$ (0.4)          | $\sim 250$ (0.3)     | [37, 38]                     |
| $^7\text{Be}$  | Cosmogenic       | 0.4                       | -                    | [37, 39]                     |
| $^{11}\text{C}$  | "                | -                         | 5.1 (1.0)            | 2.3.3, [22],<br>[40, 41, 42] |
| $^{39}\text{Ar} + ^{85}\text{Kr}$  | LAK $\text{N}_2$ | 0.1                       | -                    | [42, 43]                     |
| $^{14}\text{C}$  | Scintillator     | 1.5                       | -                    | [44]                         |
| $^{40}\text{K}$ , $K_{\text{nat}} = 10^{-14}$ g/g  | contam.          | 1.5                       | 0.4                  | 8.5.2, 9.4.2                 |
| $^{238}\text{U}$ chain $10^{-16}$ g/g  | "                | 97.5 (18.8)               | 13.1 (2.2)           | } 8.2,<br>8.4, [12]          |
| $^{232}\text{Th}$ chain $10^{-16}$ g/g   | "                | 22.9 (5.4)                | 4.0 (1.2)            |                              |
| $^{222}\text{Rn}$ daughters  | Nylon eman.      | 5.2 (0.4)                 | 1.2 (0.0)            | 4.4.3, [45]                  |
| $^{210}\text{Pb}$ daughters  | " wash-off       | 0.1 (0.0)                 | < 0.1                | } 4.4.4, 8.3,<br>[46, 47]    |
| "  | Metal w.-o.      | ?                         | ?                    |                              |
| <i>External backgrounds</i>  |                  |                           |                      |                              |
| $\gamma$ rays  | PMTs/lt.conc.    | 1.2                       | 0.8                  | } [12, 48],<br>[49]          |
| "  | Other            | 1.6                       | 0.7                  |                              |
| <i>Solar neutrinos</i>   |                  |                           |                      |                              |
| $^7\text{Be}$  | Sun              | 27.7                      | -                    | 2.3.1                        |
| $pep$  | "                | 1.3                       | 0.9                  | 2.3.3                        |
| $^{13}\text{N}$  | "                | 1.3                       | -                    | "                            |
| $^{15}\text{O}$  | "                | 1.5                       | 0.5                  | "                            |
| $^8\text{B}$   | "                | 0.1                       | [ $E > 2.8$ MeV]     | [12, 50]                     |
| <i>Other neutrinos</i> (Expected events/year in 300 tons, full spectrum)                   |                  |                           |                      |                              |
| $\bar{\nu}_e$  | Earth            | 10–24                     |                      | } 2.4.1,<br>[51, 52]         |
| $\nu_e, \bar{\nu}_e$   | Reactors         | 28                        | [8 with $E < 3$ MeV] |                              |
| $\nu_{e,\mu,\tau}, \bar{\nu}_{e,\mu,\tau}$   | 10 kpc SN        | 186 events in $\sim 10$ s |                      | 2.4.2, [53, 54]              |

Table 2.1: Summary table of expected signals and backgrounds in the Fiducial Volume (except where otherwise indicated) of Borexino. Note that as yet there is no accurate estimation for the internal scintillator contamination of  $^{40}\text{K}$  and the heavy-element chains in Borexino; the values given are for the specified assumed contaminations. The amount of contamination due to  $^{210}\text{Pb}$  wash-off from metal surfaces will depend upon their original exposure, and cannot be estimated in advance. Values in parentheses, where present, represent the reduced rates after individual event tagging methods are applied: searches for delayed coincidences,  $\alpha/\beta$  discrimination, likelihood-based tagging (this largely removes the signal from  $^{214}\text{Pb}$ ; see Section 8.4), and so on. References are to sections in this thesis or to bibliographic entries; the list is at best representative, not exhaustive.

The central part of the detector consists of 300 tons of the organic liquid pseudocumene, in which is dissolved a wavelength-shifting compound that acts both to shift the scintillation light towards the wavelength at which the photomultiplier tubes are most efficient, and to increase the total production of scintillation light. Only the central 100 tons, which comprise the region best shielded against radiation from external sources, are considered to be the target mass. Since the data collected by the detector can be analyzed to determine the approximate position of any event, as will be discussed at length in Chapter 5, it will be possible to separate out the events that occur within this most pure region. This spherical “Fiducial Volume” may be redefined at any time, as desired, by simple changes in the Borexino analysis software.

The scintillator fluid is contained within two concentric spherical vessels of thin ( $125\ \mu\text{m}$  thick), transparent nylon film. The inner vessel has a radius of about 4.25 m, and the outer vessel, 5.5 m. Both vessels are intended to prevent radioactive and highly mobile atoms of radon gas from traveling into the scintillator fluid. In addition, the inner vessel serves to separate the scintillator fluid (within it) from a buffer fluid (between the two vessels, and outside the outer one). The buffer fluid is made of pseudocumene laced with a substance that prevents scintillation. The purpose of the two volumes of buffer fluid is to shield the target mass from external radiation. They are prevented from scintillating themselves in order to keep the trigger rate of the data acquisition system at a few tens of Hz.

A large steel sphere, 6.85 m in radius, surrounds and supports the two nylon vessels. The vessels are attached to the sphere at top and bottom by steel and bulk nylon tubing. The sphere also holds about 2200 inward-pointing photomultiplier tubes. These instruments observe photons produced within the scintillator. They provide the main means by which the energy of an event may be determined.

The energy resolution of the detector is expected to follow Poisson statistics, since it is based upon the number of scintillation photons emitted by excited molecules of scintillator, and upon the fraction of those photons which both strike a photomultiplier tube and are

converted to a photoelectron. When the total number of observed photoelectrons is reasonably large (on the order of 20 or more), the energy spectrum of a monoenergetic source should closely approximate a Gaussian curve.

Borexino is expected to observe 400 photoelectrons (p.e.) for each MeV of kinetic energy released in a neutrino scattering event or radioactive  $\beta$  decay [55]. This ratio is nearly linear as long as the energy release is larger than 50–100 keV [56]. Therefore, if it were an ideal detector, the energy resolution for an event with true energy  $E$  would be given by<sup>1</sup>

$$\frac{\sigma_E}{E} = \frac{\sigma_{N_{p.e.}}}{N_{p.e.}} = \frac{1}{\sqrt{N_{p.e.}}} = \frac{k_0}{\sqrt{E}}, \quad (2.1)$$

with  $N_{p.e.}$  being the number of photoelectrons detected in the event, and the proportionality constant  $k_0 = \sqrt{(1 \text{ MeV})/(400 \text{ p.e.})} = 0.05 \text{ MeV}^{1/2}$ . Hence the expected resolution  $\sigma_E$  for 250 keV events is 25 keV (10%), and for 1 MeV events, it is 50 keV (5%). In practice the value of the proportionality constant will be greater than  $k_0$  due to light scattering, absorption, variances in photomultiplier efficiencies, and other effects. Denote the observed proportionality constant as  $k$ . For the third version of the Borexino prototype, the Counting Test Facility (CTF 3),  $k/k_0$  is found in Section 8.1.2 of this work to be 1.34. We will suppose this also to be the case for Borexino; that is, we take  $k = 0.067 \text{ MeV}^{1/2} = 2.11 \text{ keV}^{1/2}$ .

Most likely an event in which a particular kinetic energy is released will result in the detector observing a number of observed photoelectrons that corresponds to a different energy. We will call the former value  $E_r$  (“r” for “real”) and the latter value  $E_d$  (“d” for “detected”). The probability that a particle of kinetic energy  $E_r$  will be observed to produce a number of photoelectrons corresponding to kinetic energy  $E_d$  defines a resolution function  $R(E_r, E_d) dE_d$ . If we assume a Gaussian energy resolution, then  $R(E_r, E_d) = (2\pi\sigma_E^2)^{-1/2} e^{-(E_d - E_r)^2/2\sigma_E^2}$ . Substituting in Equation (2.1) gives us

$$R(E_r, E_d) = (2\pi k^2 E_r)^{-1/2} e^{-(E_d - E_r)^2/2k^2 E_r}. \quad (2.2)$$

---

<sup>1</sup>Throughout the remainder of this thesis, the kinetic energy of a particle produced by a scattering or decay event will be designated  $E$ . When it is necessary to give the total energy of a particle, including the rest mass, that quantity will be designated  $U$ . In the case of neutrinos, since their masses are negligible compared to decay energies or the electron mass, the distinction will not be made.

Suppose that in some process, a particle is given a kinetic energy in the range  $[E, E + dE]$  with probability  $\rho_r(E) dE$ . That is,  $\rho_r(E)$  is the energy spectrum of the process (again, the subscript “r” stands for “real”). It can be transformed into the form that will be observed in Borexino by a convolution with the resolution function. The convolution yields an observed energy spectrum

$$\rho_d(E) = \int_0^\infty R(E', E) \rho_r(E') dE' = (2\pi k^2)^{-1/2} \int_0^\infty \frac{\rho_r(E')}{\sqrt{E'}} e^{-(E-E')^2/2k^2 E'} dE'. \quad (2.3)$$

When the process is monoenergetic, the real energy spectrum is a  $\delta$ -function, and the observed energy spectrum becomes a Gaussian curve centered at the true event energy  $E_r$ , with width  $\sigma = k\sqrt{E_r}$ . For processes with a continuous spectrum, the convolution tends to smooth out the observed spectrum, as well as extend it slightly beyond the true high-energy end-point of the process.

## 2.2 Radioactive backgrounds

In this section we will first recall the basic types of background in Borexino, then break them down into individual isotopes and note the origin and potential danger posed by each. The section will be rather detailed since the information provided here will be used again in the final three chapters of this work.

### 2.2.1 Types of radioactive decay

A radioactive nuclide may decay in several different ways. It may emit an  $\alpha$ ,  $\beta^-$ , or  $\beta^+$  particle (these are all often accompanied by one or more  $\gamma$  rays); capture an electron from the K shell; decay by pure  $\gamma$  ray emission to a lower energy state of the same nuclide; or break apart into roughly equal-sized pieces by spontaneous fission. All of these decay methods except the last are important contributors to the background event rate in Borexino. Additionally, in Borexino, neutrons may be produced by the reaction of incoming cosmic rays or

$\alpha$  particles (themselves resulting from radioactive decay) with carbon nuclei. Since a free neutron will be captured by a proton (forming deuterium) with emission of a characteristic 2.2 MeV  $\gamma$  ray after a typical time of 250  $\mu$ s, they are not usually problematic.

Using the standard notation, consider an unspecified isotope of some element X, which has  $Z$  protons and  $N$  neutrons for a total of  $A = Z + N$  nucleons. Depending on whether  $Z$  and  $N$  are each even or odd, the isotope is classified as “even-even,” “odd-odd,” etc. Nucleons, as spin- $\frac{1}{2}$  fermions, find it energetically favorable to pair off within the nucleus. In general, therefore, even-even isotopes are the most stable, and odd-odd isotopes the least: only four odd-odd isotopes ( ${}^2\text{H}$ ,  ${}^6\text{Li}$ ,  ${}^{10}\text{B}$ ,  ${}^{14}\text{N}$ ) are stable,  ${}^2\text{H}$  only barely.<sup>2</sup>

A nucleus is subject to three of the four fundamental forces (the effect of gravity is negligible), one struggling to hold it together and the other two to tear it apart. The binding force is the residual strong interaction. Nucleons, each being composed of three quarks, are colorless objects. Yet there is still some residual attraction between them, akin to the force seen between electric dipoles that have no overall charge. This attraction is mediated by the exchange of pions. There are three types, having charges of 0 and  $\pm 1$ . (Their quark constituents are, for the  $\pi^+$ ,  $u\bar{d}$ ; for  $\pi^-$ ,  $d\bar{u}$ ; and for  $\pi^0$ ,  $(u\bar{u} + d\bar{d})/\sqrt{2}$ .) Thus they can mediate interactions between all three possible combinations  $pp$ ,  $nn$ , and  $pn$ . The residual strong interaction is short-range and acts to create a potential energy well within a nucleus.

The other forces, tending to cause radioactive decay, are electrical repulsion between the positively-charged protons, and the weak interaction that permits conversions between protons and neutrons. On one hand, as the number of neutrons is increased, the isotopes of an element become less susceptible to  $\alpha$  decay or fission caused by electrical repulsion. Adding neutrons increases the total nucleon binding energy while keeping the electrical repulsion constant. So the ratio  $N/Z$  is usually greater than one for heavy stable isotopes (reaching a maximum of about 1.5). On the other hand, if  $N$  and  $Z$  are too different, the Fermi energy level of the neutrons will be enough higher than that of the protons to make conversion of

---

<sup>2</sup>The  ${}^2\text{H}$  nucleus, or deuteron, is an interesting case. It has only one energy level, the ground state, which if excited by more than 2.22 MeV will dissociate into its component proton and neutron.

a neutron into a proton via the weak process of  $\beta$  decay energetically favorable. The two stability constraints (large  $N$  on one hand and  $N \approx Z$  on the other hand) become more and more difficult for heavy nuclei to satisfy, so there are no stable isotopes with  $Z > 83$  or  $N > 126$ .<sup>3</sup>

The difference between the mass of a radioactive isotope and the total mass of the products into which it decays is  $Q$ , the amount of energy released in the decay. This is called the  $Q$ -value; it must be greater than zero for the decay to occur. Energy released may appear as kinetic energy of the decay products, as  $\gamma$ -ray photons, or both. If more than one possible decay branch has a positive  $Q$ -value, the isotope may decay in any of these ways, with a specific probability for each.

### $\alpha$ decay

Emission of an  $\alpha$  particle, also known as the nucleus of  ${}^4\text{He}$ , is common among very heavy isotopes ( $A \sim 200$  or more). The  $\alpha$  particle, consisting of a pair of protons and pair of neutrons, is a very stable configuration. This decay mode is described by the Gamow-Condon-Gurney theory as the escape of a pre-formed  $\alpha$  particle from the nuclear potential energy well by quantum tunnelling:



The radius of the potential well, for the heavy elements that emit  $\alpha$  particles, is approximately  $R \approx 9.5$  fm for even-even isotopes [57].

Because only the  $\alpha$  particle is emitted, the decay is monoenergetic, with the  $\alpha$  having a kinetic energy almost equal to the decay's  $Q$ -value. The  $\alpha$  energy is typically in the range 4–9 MeV for heavy nuclei. The remainder of the energy goes into recoil of the nucleus, which receives a kinetic energy on the order of 100 keV in order to conserve momentum of

---

<sup>3</sup>Technically, even the single common isotope of element 83,  ${}^{209}\text{Bi}$ , is slightly radioactive, though its half-life is many times the age of the universe.

the system. An important property of  $\alpha$  decays for ultra-low background detectors is that the release of energy from them is very localized;  $\alpha$  particles will typically travel less than 0.1 mm in solid or liquid materials. Therefore one needs to worry about  $\alpha$ -decaying isotopes only in the scintillator or the vessel containing it, not in any of the other materials of the detector.

The Gamow-Condon-Gurney model can be used to show that the mean life  $\tau$  of the isotope<sup>4</sup> depends exponentially upon the Q-value of its decay, and also upon the atomic number  $Z' = Z - 2$  of the decay product:

$$\log \frac{\tau}{\tau_0} \approx Z' \sqrt{\frac{E_0}{Q}} - C\sqrt{Z'}. \quad (2.5)$$

Here,  $\tau_0 \equiv 2R/v_\alpha$  is the time it takes for the  $\alpha$  particle to travel across the original nucleus, given roughly by  $(2.74 \times 10^{-21} \text{ s})\sqrt{(1 \text{ MeV})/Q}$ . The other constants are defined by  $E_0 \equiv 8\pi^2\alpha^2 m_\alpha c^2 \approx 15.67 \text{ MeV}$  and  $C \equiv 8\sqrt{\alpha(Rm_\alpha c^2)/(\hbar c)} \approx 9.16$ . This equation, the Geiger-Nuttall relation, implies that isotopes with long half-lives emit low-energy  $\alpha$  particles ( $Q \approx 4 \text{ MeV}$ ), while very short-lived isotopes have higher-energy decays ( $Q \approx 8 \text{ MeV}$ ).

Decays by  $\alpha$  emission must of course conserve angular momentum. The  $\alpha$  particle itself has spin 0; therefore the orbital angular momentum  $\ell_\alpha$  of the  $\alpha$  must add to the spin of the daughter nucleus to yield the spin of the parent nucleus. If we write the spins of parent and daughter nuclides as  $J_i$  and  $J_f$  respectively, then the quantum mechanical rules for spin imply the inequality  $J_f + \ell_\alpha \geq J_i \geq |J_f - \ell_\alpha|$ . For an  $\alpha$  particle emitted with no angular momentum, the parent and daughter will have equal spins. In principle, however, an  $\alpha$  decay may connect any two spin states whose spins differ by an integer if the angular momentum of the  $\alpha$  particle has the requisite value.

Often connected with angular momentum is the idea of parity. This is a quantum number  $\pi$  whose value is  $+1$  for a state whose wave function is invariant under reversal of coordinate signs ( $\psi(-\mathbf{x}) = \psi(\mathbf{x})$ ), and  $-1$  for a state whose wave function changes sign under such a

<sup>4</sup>After one mean lifetime, a fraction  $1/e$  of an initial sample of radioactive atoms will remain. For this reason, the symbol “log” will always be used in this thesis to represent the *natural* logarithm.

reversal ( $\psi(-\mathbf{x}) = -\psi(\mathbf{x})$ ). These values are often abbreviated simply + and -, or even and odd, respectively. Individual particles and nuclei have their own intrinsic parities: that of the  $\alpha$  particle itself is +. Spin and parity are usually written together in the format  $J^\pi$ , for instance,  $\frac{1}{2}^+$ . The important point to note is that the spherical harmonic functions  $Y_{\ell m}$ , which describe the wave function of an  $\alpha$  particle with angular momentum  $\ell$ , have parity  $(-1)^\ell$ . Hence, for parity to be conserved in  $\alpha$  decay, the parity of the daughter nucleus must be  $(-1)^\ell$  times that of the parent. In particular, a nucleus with a ground state of  $0^+$  may decay by  $\alpha$  emission only to a daughter in one of the states  $0^+, 1^-, 2^+$ , etc.

An  $\alpha$  decay can in principle result in the daughter nucleus being in an excited state, meaning that it shortly afterwards emits one or more  $\gamma$  rays. However, all even-even isotopes have a ground state in which the nucleons are paired off with antiparallel spins. In this state, all the spins cancel: the spin and parity of the nuclide is  $0^+$ . Since  $\alpha$  decay preserves the evenness of  $N$  and  $Z$ , the product also has a ground state  $0^+$ . All other factors being equal, the  $\alpha$  particle itself is most likely to exit the parent nucleus with no angular momentum, because there is then no additional centrifugal energy barrier helping to prevent its escape. Recall also that a higher-energy  $\alpha$  decay implies a shorter half-life: the  $\alpha$  decay with the highest possible energy, that to the ground state of the daughter isotope, is thus strongly favored. As a result of these two factors, the most likely  $\alpha$  decay mode of an even-even isotope is to the ground state of the daughter, with no  $\gamma$  rays produced. This situation holds for all  $\alpha$ -decaying isotopes in the  $^{232}\text{Th}$  and  $^{238}\text{U}$  decay chains, with the single exception of odd-odd  $^{212}\text{Bi}$ . Except for decays of that isotope, only a small fraction of  $\alpha$  events in Borexino will produce  $\gamma$  rays. Since  $\gamma$  rays may travel many cm in scintillator, this fact makes  $\alpha$ -decaying isotopes useful in evaluating the position reconstruction capabilities of scintillation detectors.

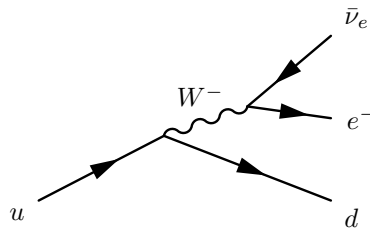
**$\beta$  decay**

$\beta$  decay, unlike  $\alpha$  decay, is a weak phenomenon. When a nucleus has too many neutrons, one neutron in the nucleus may become a proton. Odd-odd isotopes are particularly prone to this and related processes because they are converted to even-even isotopes. In  $\beta$  decay, both an electron (also called a  $\beta^-$  particle) and an electron antineutrino  $\bar{\nu}_e$  are emitted:



The electron loses all of its kinetic energy to collisions with scintillator molecules within a few cm.  $\beta$  decay is therefore observed as an essentially point-like event (the position resolution of Borexino will be on the order of 10–20 cm). Like  $\alpha$  decays, purely  $\beta$ -decaying isotopes—those which always decay to the ground state of the daughter isotope—only contribute to detector background when present in the scintillator itself or the vessel containing it. (In principle  $\beta$  decays in the volume immediately outside the vessel, if it is thin, may also contribute.)

At the quark level, a  $d$  quark emits a virtual  $W^-$ , becoming a  $u$  quark. The  $W^-$  immediately decays into an electron. A  $\bar{\nu}_e$  is also emitted in order to conserve lepton number:



Since two additional particles are produced in the decay, each of them has a continuous kinetic energy spectrum ranging from 0 up to approximately the Q-value of the decay. Their total kinetic energy is almost monoenergetic. However, the antineutrino can essentially never be observed; only the electron will be seen by the detector. If the Q-value is sufficiently high, the electron kinetic energies observed from decays of a particular isotope will be spread

across the entire energy range where one hopes to see solar neutrinos. It is ironic that this most troublesome type of background in a neutrino detector owes its intractability to the near-invisibility of neutrinos!

Often the end product of the  $\beta$  decay is an excited state of the final nuclide. It will emit one or more  $\gamma$  rays to reach the ground state. As with  $\alpha$  decay followed by an internal transition, the mean lifetime of the excited state is too short to distinguish the  $\beta$  and  $\gamma$  events.

A positron (also known as  $\beta^+$ ) may be emitted instead of an electron, with conversion of one proton in the nucleus into a neutron:



This process is very similar to “normal”  $\beta$  decay, but it cannot occur unless the Q-value of the decay would be greater than 1.022 MeV. This accounts for the  $\gamma$  rays that are produced by electron-positron annihilation immediately afterward. The maximum possible kinetic energy of the positron is thus about one MeV less than the Q-value.

The energy spectrum of the electron or positron produced in a typical  $\beta$  decay may be approximated by a phase space argument, and hence is called the statistical spectrum. The argument yields a formula for the rate of events as a function of the  $\beta$  particle momentum  $p$ . The electron or positron produced is usually relativistic. Its total energy is  $U = \gamma m_e c^2$ , and its kinetic energy is by definition  $E \equiv U - m_e c^2 = (\gamma - 1)m_e c^2$ , giving  $p^2 c^2 \equiv U^2 - m_e^2 c^4 = E^2 + 2Em_e c^2$ . The rate of events as a function of  $\beta$  kinetic energy  $E$  becomes

$$\frac{dN}{dE} = C \sqrt{E^2 + 2Em_e c^2} (E + m_e c^2) (E_{\max} - E)^2 F(Z', E). \quad (2.8)$$

Here,  $C$  is a normalization constant,  $Z'$  is the atomic number of the decay product ( $Z + 1$  for electron emission and  $Z - 1$  for positron emission), and  $E_{\max}$  equals  $Q$  for an electron or  $Q - 2m_e c^2$  for a positron.  $F$  is the Fermi function of atomic number and  $\beta$  kinetic energy. The Fermi function, a correction factor that accounts for Coulomb attraction between the

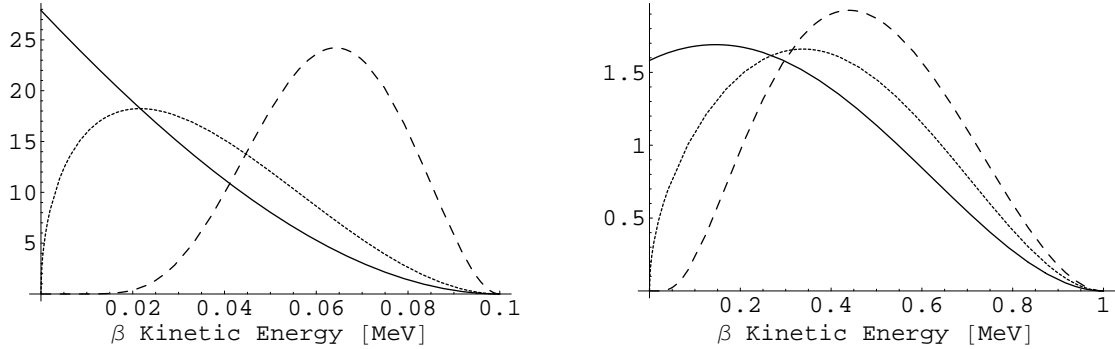


Figure 2.1: The idealized  $\beta$  particle kinetic energy spectra for two hypothetical cases in which the decay product is presumed to be an isotope of lead with an effective nuclear radius  $R = 9.5$  fm. At left, the maximum kinetic energy of the  $\beta$  is supposed to be 100 keV; at right, 1 MeV. The dotted lines are the curves obtained purely from phase space considerations without incorporating the Coulomb correction factor, Equation (2.9). The solid lines show the energy spectra for emitted electrons. At left, the shape is representative of low-energy  $\beta$  emitters such as  $^{210}\text{Pb}$ ; at right, of higher-energy  $\beta$  emitters such as  $^{210}\text{Bi}$ . The dashed lines show the spectra for emitted positrons. (These plots do not include the 1.02 MeV  $e^+e^-$  annihilation energy.) Note that the energies of the emitted electrons tend to be lower than those of the positrons due to the differences in the Coulomb force from the nucleus. These curves have been normalized such that the area under each is one, so the vertical axes are labeled in fractional probability per MeV.

nucleus and electron (or repulsion between nucleus and positron), is approximated by [58]

$$F(Z', E) = 2e^{\pi\eta} (s+1) [4\rho^2(E^2 + 2Em_e c^2)]^{s-1} \left| \frac{\Gamma(s+i\eta)}{\Gamma(2s+1)} \right|^2, \quad (2.9)$$

$$\rho \equiv \frac{m_e c^2}{\hbar c} R$$

$$s \equiv \sqrt{1 - (\alpha Z')^2}$$

$$\eta \equiv \pm \alpha Z' \frac{E + m_e c^2}{\sqrt{E^2 + 2Em_e c^2}} \text{ for } e^{(\mp)}.$$

The  $\Gamma$  function is the continuous generalization of the factorial over the complex plane; for integer  $n$ ,  $\Gamma(n) \equiv (n-1)!$  Figure 2.1 shows the energy spectra predicted by Equations (2.8) and (2.9), for hypothetical  $\beta$  decays by electron and positron emission to a product with atomic number  $Z' = 82$  (lead) and effective nuclear radius  $R = 9.5$  fm.

Most commonly the  $\beta$  decay of a nuclide with specific spin and parity  $J^\pi$  will yield another nuclide with the same parity, whose spin differs by 0 or  $\pm 1$ . This is an “allowed decay.” The reason for this is the requirement to conserve angular momentum. Suppose for the moment that the total orbital angular momentum of the three products (the two leptons and the daughter nucleus) is zero, as is the most probable situation. The electron and antineutrino each have a spin of  $\frac{1}{2}$ , and therefore have a combined angular momentum of either 0 or 1. In the former case, a “Fermi transition,” the parent and daughter nucleus must have the same spin. In the latter case, a “Gamow-Teller transition,” the spin of the daughter may differ from that of the parent by  $\Delta J = \pm 1$ ; or, if the spin of the parent is not zero, may be the same as that of the parent. Note that if the parent and daughter have the same spin, and that spin is non-zero, the decay may be a linear combination of Fermi and Gamow-Teller transitions.

For some isotopes, the nuclear structure of the possible  $\beta$  decay products is such that neither a Fermi nor Gamow-Teller transition may occur. In this case the parent nucleus, in order to decay, must emit an electron and antineutrino pair with a non-zero total orbital angular momentum. This situation is kinematically disfavored; such decays are suppressed, usually by at least two orders of magnitude, relative to allowed decays. The transition is called  $n^{\text{th}}$ -order forbidden if  $\Delta J = \pm n$  or  $\pm(n+1)$  and the product of parent and daughter nuclide parities is  $\pi_i \pi_f = (-1)^n$ . The possible second-forbidden transitions, for instance, have  $\Delta J = \pm 2, \pm 3$  with no parity change. First-forbidden transitions (which do exhibit a parity change), in addition to the expected spin changes  $\Delta J = \pm 1, \pm 2$ , may also have no spin change,  $\Delta J = 0$ .

The difference in the energy spectrum for an  $n^{\text{th}}$ -order forbidden transition with respect to an allowed decay is given by a shape factor  $S_n(Z', E)$ . In general this factor depends upon ratios of nuclear matrix elements as well as kinematic variables. But for  $n^{\text{th}}$ -order forbidden decays with  $\Delta J = \pm(n+1)$ , called “unique decays,” only one matrix element is involved. It can in this case be absorbed into the overall normalization coefficient. For example, the

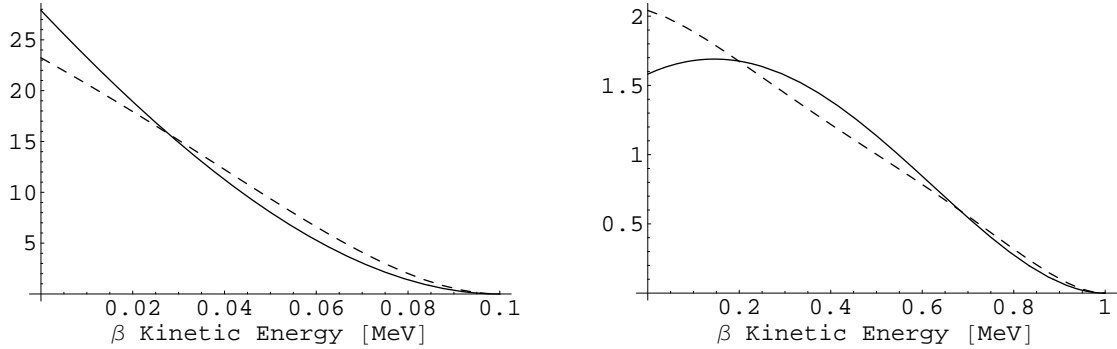


Figure 2.2: The idealized  $\beta$  particle kinetic energy spectra for two hypothetical cases in which the decay product is presumed to be an isotope of lead with an effective nuclear radius  $R = 9.5$  fm. At left, the maximum kinetic energy of the  $\beta$  is supposed to be 100 keV; at right, 1 MeV. The solid lines show the energy spectra for an allowed  $\beta^-$  decay; the dashed lines show the spectra for a unique first-forbidden  $\beta^-$  decay, Equation (2.10). These curves have been normalized such that the area under each is one.

shape factor for the unique first-forbidden transition ( $\Delta J = \pm 2; \pi_i \pi_f = -1$ ) is [59]

$$S_{1\Gamma}(Z', E) = \frac{(s+1)}{24m_e^2c^4} [(E_{\max} - E)^2 + A(Z', E)(E^2 + 2Em_e c^2)] \quad (2.10)$$

where

$$A(Z', E) \equiv \frac{s_1 + 2}{2s + 2} \left( \frac{12\Gamma(2s + 1)}{\Gamma(2s_1 + 1)} \right)^2 [4\rho^2(E^2 + 2Em_e c^2)]^{s_1 - s - 1} \left| \frac{\Gamma(s_1 + i\eta)}{\Gamma(s + i\eta)} \right|^2$$

$$s_1 \equiv \sqrt{4 - (\alpha Z')^2}$$

and the symbols  $s, \eta, \rho$  have the same meanings as in Equation (2.9). The spectra for hypothetical 1-MeV and 100-keV unique first-forbidden decays are compared to spectra for allowed transitions in Figure 2.2. It is also worth noting that the spectra of *non*-unique first-forbidden  $\beta$  decays are usually closely approximated by the statistical shape of Equation (2.8).

### Electron capture

It may be energetically favorable for an isotope to convert one of its protons to a neutron, but with a Q-value of less than 1.022 MeV. In this case  $\beta^+$  decay is not possible. The nucleus may instead capture an electron from an inner orbital of its electron cloud:



A decay of this type is called electron capture (symbolized  $\varepsilon$ ). It may occur even when the Q-value is greater than 1.022 MeV, in competition with positron emission.

Unless the daughter isotope is produced in an excited state, electron capture is invisible to scintillation detectors because nearly all of the energy released is carried away by the neutrino. The slight kinetic energy imparted to the daughter nucleus, the nuclear recoil, is on the order of 1–10 eV, far below the thresholds of Borexino and similar detectors.

### $\gamma$ emission

Any of the decay modes  $\alpha$ ,  $\beta^\pm$ ,  $\varepsilon$  may produce a daughter isotope in an excited state. These excited states are called isomers. They usually decay to the ground state by emitting one or more  $\gamma$  rays. Therefore all energy released by a decay, except that bound up in neutrinos, may in principle be observed by the detector. Typically the half-life of the isomer is less than 1 ns, so the  $\gamma$  rays are inextricable from the parent isotope decay in the observed scintillation light. In some cases the parent isotope may decay to several different excited states of the daughter, as with the decay of  ${}^{214}\text{Bi}$ , resulting in a very complex energy spectrum. Each component of the spectrum consists of a pure  $\beta$  decay spectrum, shifted to higher energies by the energy of the associated  $\gamma$  rays.

Because  $\gamma$  rays may travel tens of cm through the Borexino scintillator, isotopes whose decay results in the production of high-energy  $\gamma$  rays are very problematic for the detector. The higher in energy the  $\gamma$  rays are, the farther they are likely to travel. Some isotopes

| Species                 | Decay mode             | Q value [MeV] | Half-life $\tau_{1/2}$ | Source       | Method of exclusion    |
|-------------------------|------------------------|---------------|------------------------|--------------|------------------------|
| $\mu^\pm$               | various                | large         | -                      | Cosmic rays  | Inner and Outer MVS    |
| $n$                     | $p(n, \gamma)d$        | 2.223         | 178 $\mu$ s            | Cosmogenic   | MVS and time cut       |
| ${}^7\text{Be}$ (10%)   | $\varepsilon + \gamma$ | 0.478         | 53.3 d                 | Cosmogenic   |                        |
| ${}^{11}\text{C}$       | $\beta^+$              | 1.982         | 20.4 m                 | Cosmogenic   | MVS, time/spatial cuts |
| ${}^{14}\text{C}$       | $\beta^-$              | 0.156         | 5730 yr                | Scintillator | Energy cut             |
| ${}^{39}\text{Ar}$      | $\beta^-$              | 0.565         | 269 yr                 | Air          |                        |
| ${}^{40}\text{K}$ (89%) | $\beta^-$              | 1.312         | 1.28 Gyr               | Dust         |                        |
| ${}^{40}\text{K}$ (11%) | $\varepsilon + \gamma$ | 1.461         |                        |              |                        |
| ${}^{85}\text{Kr}$      | $\beta^-$              | 0.687         | 10.7 yr                | Air          |                        |
| ${}^{87}\text{Rb}$      | $\beta^-$              | 0.273         | 47.5 Gyr               | Dust         |                        |

Table 2.2: Summary table of potentially problematic lower-mass radioactive species in Borexino. The Q value for  ${}^{11}\text{C}$  includes the electron/positron annihilation energy following  $\beta^+$  decay. For decays by electron capture, only the energy of any emitted  $\gamma$  ray is given. MVS stands for Muon Veto System.

may produce  $\gamma$  rays that travel all the way into the Fiducial Volume from the scintillator containment vessels and even from the photomultiplier tubes (a distance of over 3 m). Most of these  $\gamma$  rays are already reduced in energy when they enter the scintillator; they are observed as a continuous energy spectrum whose details may be calculated only by Monte Carlo simulations. Furthermore, because  $\gamma$  rays deposit energy in several different places within the scintillator, the reconstructed position of a  $\gamma$ -ray-producing event will be much less accurate than that of a pure  $\alpha$  or  $\beta$  decay.

In a few cases an isomer lasts significantly more than a nanosecond. It may then be designated by an “m” attached to the atomic number in the isotope symbol. For instance, the  $\beta$ -decaying isotope  ${}^{85}\text{Kr}$  decays into the excited state  ${}^{85\text{m}}\text{Rb}$  with 0.4% probability;  ${}^{85\text{m}}\text{Rb}$ , with a half-life of 1.01  $\mu$ s, then emits a 514 keV  $\gamma$  ray to reach the ground state of  ${}^{85}\text{Rb}$ .

### 2.2.2 The isotopes present in Borexino

The isotopes with the potential to cause problems for Borexino data analysis may be broken down into several categories. There are naturally occurring, long-lasting radioactive isotopes such as  $^{40}\text{K}$  and  $^{87}\text{Rb}$ . Less long-lived isotopes may still be found because they are continually recreated in matter by the impact of cosmic rays, as with  $^{14}\text{C}$ , or byproducts of human activities, such as  $^{85}\text{Kr}$ . Cosmic rays may penetrate to the detector itself during operation, leaving behind short-lived cosmogenic isotopes such as  $^{11}\text{C}$ . Finally, three long-lived naturally occurring isotopes each form the head of a long and complex decay chain involving over a dozen species.

#### The special problem of radiocarbon

The  $\beta^-$ -decaying isotope  $^{14}\text{C}$  is by far the largest source of background in a detector based on organic scintillator. This isotope is cosmogenic. At the surface of Earth, the  $^{14}\text{C}$  concentration in air is continually renewed by the interaction of cosmic rays with carbon dioxide gas in the upper atmosphere. Since the half-life is relatively long—5730 years—the concentration that builds up is not negligible. Indeed, it forms the basis of radiocarbon dating. During life, all organisms respire, metabolizing  $\text{CO}_2$  into their genetic and structural makeup. At death, respiration ceases, so the amount of  $^{14}\text{C}$  left in the remains follows an exponential decay curve. It is therefore possible (with some difficulty, due to long-term variations in atmospheric  $^{14}\text{C}$  levels) to determine the ages of materials derived from living things (bone, ivory, wood, fabric, etc.) as long as they are not too recent or too old.

This panacea for archaeologists presents a grave problem to low-background physics experiments, such as Borexino, that are based on an organic scintillator. Unlike most contaminants,  $^{14}\text{C}$  cannot be removed by purification as it is chemically indistinguishable from stable carbon, and present in molecules of the scintillator itself. (The other such radioisotope one might conceivably worry about,  $^3\text{H}$  or tritium, decays by  $\beta^-$  emission with a

Q-value of 19 keV, which is at the detector’s low-energy threshold.) In natural air, the mass ratio of  $^{14}\text{C}$  to  $^{12}\text{C}$  is on the order of  $10^{-12}$  g/g. If the Borexino scintillator contained  $^{14}\text{C}$  at this isotopic ratio, it would exhibit a  $^{14}\text{C}$  activity of 150 Bq per kg of scintillator.

Fortunately, the Borexino scintillator (like most commercially manufactured organic materials) is derived from petroleum. Petroleum products have spent millions of years deep underground, protected from cosmic rays; the  $^{14}\text{C}$  isotopic abundance measured in the scintillator was only  $(5 \pm 2) \times 10^{-18}$  g/g [44]. Nevertheless, this implies an activity of  $0.75 \pm 0.3$  mBq/kg of scintillator, for a total expected  $^{14}\text{C}$  event rate in the Fiducial Volume of  $75 \pm 30$  Bq, or 6.4 million events/day. It will be impossible to separate any neutrino events below or (due to finite energy resolution) within 50–100 keV of the end-point from this enormous background. The Q-value for the  $^{14}\text{C}$   $\beta$ -decay is 156 keV. Taking into account the finite energy resolution of the detector as in Section 2.1, we predict that the rate of  $^{14}\text{C}$  events in the Fiducial Volume with an observed energy  $> 250$  keV will be 0.35 events/day. If the energy threshold is lowered to 240 keV, this rate grows to 1.9 events/day, and at 230 keV, to 8.8 events/day. See Figure 2.3.

A second concern is the fact that if two  $^{14}\text{C}$  decays occur in close proximity in time, they may look like a single higher-energy event (“pile-up”). For this to happen, they must occur within an interval short enough that the event pulse shapes summed over PMTs (as functions of time) overlap. The scintillator volume has a diameter of 8.5 m and therefore it takes a scintillation photon (in a fluid with a refractive index of 1.5) about 43 ns to cross it. Hence light from an event at the edge of scintillator will reach the most distant PMT 43 ns after it reaches the nearest. Also taking into account the time distribution of the scintillator response function (refer to Section 7.5) and the additional delays introduced by scattering effects, we may estimate the maximum pulse duration to be no more than 80 ns. The expected rate of pairs of  $^{14}\text{C}$  events within the Fiducial Volume that occur within 80 ns is 38 per day; for two  $^{14}\text{C}$  events anywhere in the scintillator, it is 344 per day. (A factor of 3 increase in mass implies the same increase in individual event rate, for a factor of  $3^2$  increase in pile-up event rate).

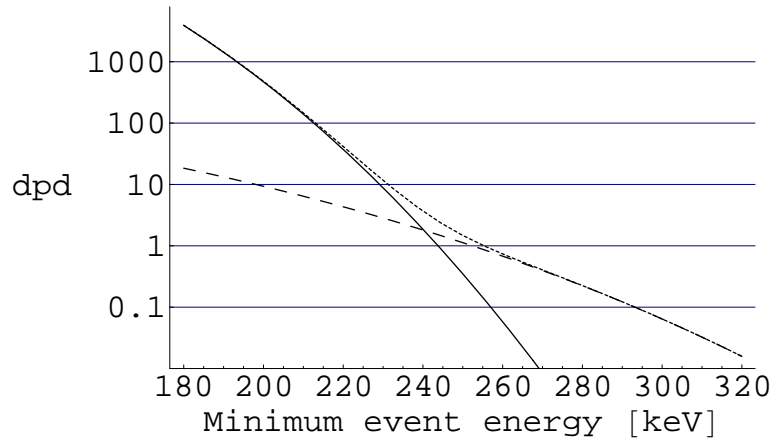


Figure 2.3: The total rate of  $^{14}\text{C}$  events in the Borexino Fiducial Volume, in decays/day (dpd), as a function of the lower limit of the energy range under study. (That is, the function shown represents the integral of the  $^{14}\text{C}$  energy spectrum above each given energy.) The solid line represents individual  $^{14}\text{C}$  events, while the dashed line represents two  $^{14}\text{C}$  events that occur sufficiently close together in time to be detected as a single higher-energy event, a phenomenon called “pile-up.” The dotted line is their sum. This figure incorporates the finite energy resolution of the detector; the actual  $^{14}\text{C}$  spectrum end-point is 156 keV, off the left edge of the graph.

The reconstructed position estimates that will be obtained for such double events are not meaningful. If the reconstructed position is completely random, it statistically should have a probability of roughly  $\frac{1}{3}$  of lying within the Fiducial Volume, giving about 120 pile-up events/day that pass the volume cut. However, if it is approximately given by the average of the positions of the two individual decays, it will have a probability more like 80% of being inside the Fiducial Volume, for about 275 pile-up events/day that pass the volume cut. To determine which value is more correct would likely require a full Monte Carlo simulation of the detector. To be conservative, we use the higher figure here. Nevertheless, it is possible that a large fraction of pile-up events may be rejected by some method, for instance, with a cut on the goodness of fit of the reconstructed event position.

The fraction  $f$  of pile-up events that will appear to have a total kinetic energy greater than a given value  $\mathcal{E}$  is

$$\begin{aligned}
f &= \int_{E=0}^{\infty} \text{P}(E_1 \in [E, E + dE]) \text{P}(E_2 > \mathcal{E} - E_1) \\
&= \int_0^{\infty} dE \rho(E) \int_{\mathcal{E}-E}^{\infty} dE' \rho(E'),
\end{aligned} \tag{2.12}$$

where  $\rho(E)$  is the observed kinetic energy spectrum of the emitted electron in Borexino. To be precise,  $\rho(E)$  is not the same as the ideal spectrum; it also takes into account the finite energy resolution of the detector and the reduced detector efficiency for observing very low-energy events (below about 50 keV). However a conservative estimate may be obtained by ignoring the detector efficiency at low energies, and using for  $\rho(E)$  the function of Equation (2.8) convoluted with the detector energy resolution as in Equation (2.3). Doing so, and integrating numerically, gives  $f = 0.13$  when  $\mathcal{E}$  is set to the  $^{14}\text{C}$  end-point of 156 keV. Setting  $\mathcal{E}$  to the lower end of the neutrino window, 250 keV, yields  $f = 0.004$ . Therefore the rate of these overlapping events within the neutrino window should not be greater than  $275 \times 0.004 \approx 1.1$  per day in the Borexino Fiducial Volume, weighted heavily toward the lower energy bound. It should be emphasized, though, that this value is proportional to the square of the  $^{14}\text{C}$  contamination. If it is only a factor of three worse in Borexino than the value measured in the Counting Test Facility, the lower neutrino window end-point would have to be increased by as much as 40 keV.

### Other light cosmogenic isotopes

The observed event rate in Borexino due to the isotope  $^{14}\text{C}$  will be essentially constant over time due to its long half-life. However, because of the depth of the experiment underground,  $^{14}\text{C}$  will not be regenerated at a rate comparable to its decay. The same cannot be said for some other, shorter-lived, cosmogenic isotopes. Those that are most potentially problematic in Borexino include  $^7\text{Be}$  and  $^{11}\text{C}$ . Other isotopes produced by muon interactions with the organic scintillator fluid all have half-lives of at most 15 s, and Q-values greater than

10 MeV. Muons can be detected with 99.98% efficiency by the Borexino muon veto system (Section 3.3.2). When a muon is observed to pass through the detector, events following within a few seconds may be excluded from the data sample. Furthermore, most decays of these other isotopes will have an observed  $\beta$  energy far greater than the upper limit of the interesting energy range.

The isotope  ${}^7\text{Be}$  has a half-life of 53.3 d, so cannot be excluded by a muon coincidence cut. It decays by electron capture, but 10.4% of the time, it reaches an excited state of  ${}^7\text{Li}$  which emits a monoenergetic 478 keV  $\gamma$  ray, right in the middle of the neutrino energy window. The predicted  $\sigma_E$  at this energy is 46 keV, so it could potentially obscure a region of spectrum about 100 keV wide in the neutrino energy window. However, the expected event rate is only 0.4 events/day within the Fiducial Volume [42]. It should therefore not pose a big problem.

The cosmogenic  ${}^{11}\text{C}$  has a half-life of 20.4 min. It decays by  $\beta^+$  emission, with a Q-value of 1.982 MeV. Hence the observed energy of the decay is always between 1.022 and 1.982 MeV. Though no problem for observing  ${}^7\text{Be}$  neutrinos, this range overlaps an interesting energy region at 0.8–1.3 MeV where the *pep* solar neutrinos could potentially be observed. Furthermore,  ${}^{11}\text{C}$  will be produced within the Fiducial Volume at a rate of  $15 \pm 2$  events/day; 35% of these decays will fall into the *pep* energy range [42]. Considerable effort has gone into the study of the production of this isotope, therefore [22, 40, 41, 42].

Through detailed simulations, it was determined that in 95% of cases, the cosmogenic production of a  ${}^{11}\text{C}$  atom is accompanied by emission of a neutron. (The other 5% are “invisible channels” through which the  ${}^{11}\text{C}$  production cannot be readily detected.) The neutron is easily seen when it is captured by a hydrogen atom, yielding deuterium with production of a 2.2 MeV monoenergetic  $\gamma$  ray. The time scale for this process is  $\tau = 257 \pm 27 \mu\text{s}$  [41]. A spherical volume, centered about the reconstructed position of the neutron capture, is defined, and this volume is monitored for likely  ${}^{11}\text{C}$  decays for several half-lives. The  ${}^{11}\text{C}$  rate may be reduced to about 20% of its original value while retaining

93% of the *pep* neutrino data sample simply by excluding these “dead” volumes surrounding each neutron capture event for several  $^{11}\text{C}$  mean lives [40]. This gives a signal-to-background ratio for *pep* neutrinos compared to  $^{11}\text{C}$  events of  $S/B = 0.9$  [22]. The optimum values of the cuts in this case are  $r < 76$  cm and  $t < 108$  min [22]. Of course, the  $^{11}\text{C}$  rate may be reduced further (asymptotically to 5%) at the cost of losing more neutrino data sample by increasing the cut radius or wait time. If the  $^{11}\text{C}$  decay can be positively identified within the dead volume, or if the dead volume can be reduced by also reconstructing the path of the progenitor muon, the neutrino sample loss may be mitigated.

### Radioactive noble gases

Three noble gas isotopes, present in all unpurified air, are of particular concern in Borexino. These are  $^{39}\text{Ar}$ ,  $^{85}\text{Kr}$ , and  $^{222}\text{Rn}$ . The first two of these are  $\beta^-$  emitters; they produce decays which are essentially indistinguishable from neutrino scattering events. The last,  $^{222}\text{Rn}$ , decays by  $\alpha$  emission, so it can be identified with  $\alpha/\beta$  discrimination techniques, but it produces a long series of even more radioactive daughters.  $^{222}\text{Rn}$  and its daughters will be described further in a later section.

The isotope  $^{39}\text{Ar}$  is produced, like  $^{14}\text{C}$ , by cosmic rays interacting with stable isotopes in the Earth’s atmosphere. It has a half-life of 269 yr, and is present in normal air at a concentration of 13 mBq/m<sup>3</sup> at STP [60]. Purified argon gas (present in air at a volume fraction of 0.93%) therefore has an intrinsic activity of 1.4 Bq/m<sup>3</sup>. It is a  $\beta^-$  emitter, with a Q-value of 565 keV, and decays by a unique first-forbidden transition directly to the  $^{39}\text{K}$  ground state (no accompanying  $\gamma$  rays). There is no way to distinguish decays of the isotope from neutrino scattering events in Borexino, so it is a very dangerous contaminant.

The requirement set for  $^{39}\text{Ar}$  activity in Borexino is no more than one event per day (0.1  $\mu\text{Bq}/\text{m}^3$ ) in the Fiducial Volume. To reach this goal, the Borexino nylon vessels are in the process of being purged repeatedly, first with high-purity nitrogen, and eventually

with special Low Argon-Krypton (LAK) nitrogen. Given equal volumes of nitrogen gas and pseudocumene liquid, argon will partition itself between the two in a ratio of 4.1:1 [43]. Therefore, the volume fraction of argon in the LAK nitrogen must be no greater than  $3 \times 10^{-7}$ , a reduction factor of  $3 \times 10^4$  from that in normal air.

The isotope  $^{85}\text{Kr}$ , on the other hand, is anthropogenic; it is released from nuclear fuel reprocessing plants. The half-life is 10.8 yr, and the Q-value is 687 keV. Like  $^{39}\text{Ar}$ , it decays by  $\beta^-$  emission to the ground state of the daughter isotope (in this case,  $^{85}\text{Rb}$ ) via a unique first-forbidden transition. Its decays are similarly indistinguishable from neutrino events, and the spectra of the two isotopes within the neutrino window look quite similar.

The activity of air due to  $^{85}\text{Kr}$  is currently  $\sim 1 \text{ Bq/m}^3$ , and slowly increasing. Hence the activity of pure krypton gas (found in air at volume fractions near  $10^{-6}$ ) is on the order of  $10^6 \text{ Bq/m}^3$ . With a partitioning ratio for krypton between nitrogen and air of 1.3:1, the volume fraction of krypton in Borexino's LAK nitrogen must be less than about  $10^{-13}$ . This is a factor of  $10^7$  less than in air.

There is one method by which the rate of  $^{85}\text{Kr}$  decays may in principle be directly measured. With 0.43% probability, an atom of  $^{85}\text{Kr}$  may decay into an excited state of  $^{85}\text{Rb}$ . This excited state, known as  $^{85\text{m}}\text{Rb}$ , has a half-life of 1.01  $\mu\text{s}$  before emitting a monoenergetic 514 keV  $\gamma$  ray to reach the nuclear ground state. This short-lived excited state makes it possible to look for "coincidences" in which two events that occur within a few  $\mu\text{s}$  have the correct energies ( $E_1 < 173 \text{ keV}$ ,  $E_2 \approx 514 \pm 50 \text{ keV}$ ). The rate of such coincidences can be extrapolated to estimate the rate of all  $^{85}\text{Kr}$  decays in the Fiducial Volume.

It should be noted, though, that if the  $^{85}\text{Kr}$  activity meets the goal of one event per day in the Fiducial Volume, the number of these coincidences observed throughout the scintillator during the ten-year lifetime of the Borexino experiment will be only  $48 \pm 7$ . The method is not very sensitive at all. Because the first event of the coincidence falls into the energy range dominated by  $^{14}\text{C}$ , it will also be susceptible to false positives. For instance, the number of accidental coincidences caused by a  $^{14}\text{C}$  event followed within 3  $\mu\text{s}$  by a neutrino

event within  $1\sigma$  of 514 keV will be about  $54 \pm 7$  over ten years. (This assumes a neutrino event rate of 22 events/day in the range  $514 \pm 50$  keV over the entire volume of scintillator.)

The Borexino experiment has found commercial suppliers of liquid nitrogen that improves upon the required argon contamination by factors ranging from 10–600 [43], and upon the required krypton contamination by up to a factor of three [42]. It is thought, therefore, that these two noble gas isotopes represent a solved problem. Great care is required nonetheless. A  $30 \text{ cm}^3$  bubble of outside air that somehow entered the scintillator would exceed the requirement for krypton all by itself; an air bubble ten times larger (still only a third of a liter) would seriously damage the sensitivity of the experiment.

### Medium-weight long-lived isotopes

The category of long-lived isotopes includes those that are no longer being generated on Earth by any important mechanism, but which have survived since the origin of the solar system due to their exceedingly long half-lives. Here we mention only those that decay immediately to stable products. The heavy-element decay chains will be described later. As metals, these isotopes may be found in dust particles, or simply be present as dilute solutions within the scintillator.

One isotope in this family is  $^{87}\text{Rb}$ , a pure  $\beta^-$  emitter that decays via a non-unique third-forbidden transition. The abundance of rubidium in the Earth's crust is roughly 78 ppm by weight [61], and the isotopic abundance of  $^{87}\text{Rb}$  is 28%. Combined with the isotope's half-life of 47 billion years, its expected activity in typical rock dust is about 65 mBq/kg. However, the Q-value of the decay is only 273 keV. The majority of decays will yield a  $\beta$  energy well below the neutrino energy window starting at 250 keV, therefore, and this isotope is not considered much of a concern.

More problematic is  $^{40}\text{K}$ . This isotope decays by pure  $\beta^-$  emission (in a unique third-forbidden transition) with 89.3% probability. The abundance of potassium in the upper

crust of the Earth is 2.7% by weight [62], with an isotopic abundance for  $^{40}\text{K}$  of 117 ppm. The half-life is 1.28 billion years, implying a total activity in rocky material of 810 mBq/kg, more than ten times that of  $^{87}\text{Rb}$ . Furthermore, its  $\beta$  spectrum endpoint is 1.312 MeV, so it produces events throughout the neutrino energy range.

It will be possible, and fairly easy, to get a good measurement of the amount of  $^{40}\text{K}$  in the Borexino scintillator. This is because the other decay branch (10.7% probability) is an electron capture yielding  $^{40}\text{Ar}$ . (Though positron emission is energetically possible, it occurs very rarely, with a branching ratio of 0.001%.) Nearly all of the time (98%), the  $^{40}\text{Ar}$  nucleus is produced in an excited state, and immediately emits a monoenergetic 1.46 MeV  $\gamma$  ray that is easily visible in the energy spectrum. (This measurement is performed for the prototype Counting Test Facility in Sections 8.5.2 and 9.4 of this work, with inconclusive but somewhat worrying results.) The presence of this  $\gamma$  ray also, however, means that potassium in structural components of the detector, external to the scintillator, may produce an additional  $\gamma$ -ray background within the Fiducial Volume.

The maximum concentration of potassium (all isotopes) considered acceptable in the Borexino scintillator is on the order of  $10^{-14}$  grams per gram of scintillator. This contamination level yields 1.5 events/day in the Borexino Fiducial Volume at  $^7\text{Be}$  neutrino energies, 250–800 keV [12].

Two  $\beta$ -emitting rare earths,  $^{138}\text{La}$  and  $^{176}\text{Lu}$ , also fall into the category of long-lived natural radioisotopes. Each of these has an expected activity in rock on the order of  $30 \mu\text{Bq/kg}$ , though, so their contributions to radioactive background in Borexino should be negligible. The radioactive heavy metals (uranium and thorium) present many more difficulties.

### 2.2.3 The heavy element decay chains

There are three naturally occurring heavy decay chains. Within each chain, every isotope has the same atomic number, modulo four (both  $\alpha$  and  $\beta$  decay preserve this modulus).

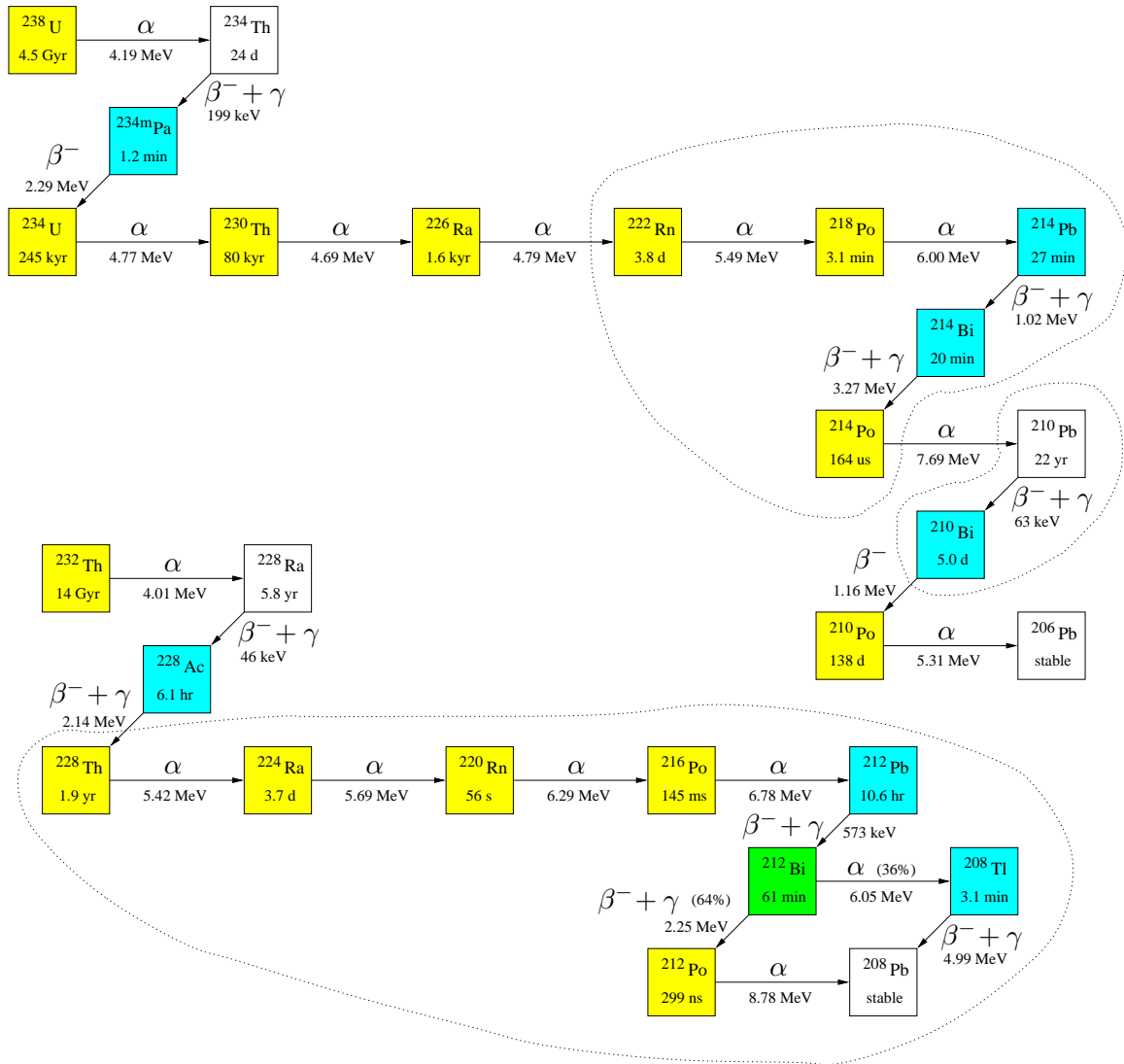


Figure 2.4: Pictorial representations of the  $^{238}\text{U}$  and  $^{232}\text{Th}$  decay chains. Secular equilibrium is likely to hold only within the sets of isotopes grouped by dotted lines. Energies shown are Q values for  $\beta$  emitters, and  $\alpha$  kinetic energy for  $\alpha$  emitters. Times shown are half-lives. Isotopes shaded blue are  $\beta$  emitters with a spectrum endpoint above the 250 keV lower limit of the neutrino energy window. They are most problematic. Isotopes shaded yellow are  $\alpha$  emitters. Due to  $\alpha$  quenching in the scintillator (Section 3.1.2), their decays cause scintillation events that appear to have energies in the neutrino window. However they may be excluded from the neutrino data sample via pulse shape discrimination with an efficiency of about 95%.  $^{212}\text{Bi}$  is shaded green as it decays both by  $\alpha$  and by  $\beta$  emission.

Like  $^{40}\text{K}$ , the parent isotope of each chain has a sufficiently long lifetime that some amount remains from the origin of the solar system. The uranium series, whose parent is  $^{238}\text{U}$ , is the  $A = 4n + 2$  chain; the thorium series, whose parent is  $^{232}\text{Th}$ , is the  $4n$  chain; the actinium series, whose parent is  $^{235}\text{U}$ , is the  $4n + 3$  chain. The  $4n + 1$  chain, or neptunium series, does not include any progenitor long-lived enough to survive until the present day. Even isotopes in the actinium series are rare enough that they present no problem to Borexino (but see Section 8.2.3). The uranium and thorium series are depicted in Figure 2.4.

Many nuclides in these decay chains decay by  $\alpha$  emission at high energies. Due to the phenomenon of  $\alpha$  quenching, unfortunately, nearly all of these will be observed to have  $\beta$ -equivalent energies within the neutrino energy window. But most (90–95%) will be possible to exclude from the data sample by means of the  $\alpha/\beta$  discrimination techniques discussed in Section 8.1.3.

### The uranium series

The uranium series isotopes are as follows. Refer to Figure 2.4 or Table 2.3 for their decay energies and half-lives.

$^{238}\text{U}$ , an  $\alpha$ -emitter, is the progenitor of the chain. It is present in typical rock dust at 2.5 ppm by weight, resulting in an activity of 30 mBq/kg [62]. Although less than that of  $^{40}\text{K}$  by a factor of nearly 30, this activity must be multiplied by the number of daughter isotopes (14) when  $^{238}\text{U}$  is in secular equilibrium with them.

$^{234}\text{Th}$  is not a problem due to its low Q-value (199 keV). It always decays to an isomer called  $^{234\text{m}}\text{Pa}$  of its daughter isotope.

$^{234\text{m}}\text{Pa}$  is peculiar in that it nearly always (99.87%) decays by  $\beta$  emission rather than relaxing to the isotopic ground state. The decay mode is pure  $\beta^-$  with 2.29 MeV end-point. Hence many of its decays are observed within the neutrino energy window.

| Species                         | Decay mode | Q value [MeV] | $E_\alpha$ or $E_{\beta+\nu}$ [MeV] | $E_\gamma$ [MeV] | Branching ratio [%] | Half-life $\tau_{1/2}$ |
|---------------------------------|------------|---------------|-------------------------------------|------------------|---------------------|------------------------|
| $^{238}\text{U}$                | $\alpha$   | 4.270         | 4.196                               | -                | 77                  | 4.47 Gyr               |
| $^{234}\text{Th}$               | $\beta^-$  | 0.199         | 0.199                               | -                | 72                  | 24.1 d                 |
| $^{234\text{m}}\text{Pa}$       | $\beta^-$  | 2.29          | 2.29                                | -                | 98                  | 1.18 m                 |
| $^{234}\text{U}$                | $\alpha$   | 4.856         | 4.774                               | -                | 72                  | 245 kyr                |
| $^{230}\text{Th}$               | $\alpha$   | 4.771         | 4.687                               | -                | 76.3                | 80 kyr                 |
| $^{226}\text{Ra}$               | $\alpha$   | 4.871         | 4.785                               | -                | 94.5                | 1600 yr                |
| <i>Radon 222 and daughters:</i> |            |               |                                     |                  |                     |                        |
| $^{222}\text{Rn}$               | $\alpha$   | 5.591         | 5.490                               | -                | 99.9                | 3.82 d                 |
| $^{218}\text{Po}$               | $\alpha$   | 6.115         | 6.002                               | -                | $\sim 100$          | 3.05 m                 |
| $^{214}\text{Pb}$               | $\beta^-$  | 1.024         | 0.672                               | 0.352            | 48                  | 26.8 m                 |
| $^{214}\text{Bi}$               | $\beta^-$  | 3.270         | 1.51                                | 1.76             | 40                  | 19.7 m                 |
| $^{214}\text{Po}$               | $\alpha$   | 7.833         | 7.687                               | -                | $\sim 100$          | 164 $\mu\text{s}$      |
| $^{210}\text{Pb}$               | $\beta^-$  | 0.063         | 0.016                               | 0.047            | 81                  | 22.3 yr                |
| $^{210}\text{Bi}$               | $\beta^-$  | 1.161         | 1.161                               | -                | $\sim 100$          | 5.01 d                 |
| $^{210}\text{Po}$               | $\alpha$   | 5.408         | 5.305                               | -                | $\sim 100$          | 138.4 d                |
| $^{206}\text{Pb}$               | stable     |               |                                     |                  |                     |                        |

Table 2.3: Summary table of the Uranium-238 decay chain. The energy carried by the  $\alpha$  particle or  $\beta$  and neutrino, and the total energy released in  $\gamma$  rays, respectively, are shown for the decay mode with the greatest branching ratio.

$^{234}\text{U}$  is another  $\alpha$  emitter, as are daughters  $^{230}\text{Th}$  and  $^{226}\text{Ra}$ .

$^{222}\text{Rn}$ , another  $\alpha$  emitter, is a special isotope. As a noble gas, atoms of this element are seldom found ionized; they are free to diffuse through most materials. It may travel long distances during its lifetime ( $\tau_{1/2} = 3.8$  days). When it does, this breaks secular equilibrium in the decay chain. The concentration of radon in a volume is no indication that it contains an equal activity of the higher isotopes. In Borexino, in particular, radon produced by the decay of radium in the nylon vessels, steel support structures, photomultipliers, or even steel sphere may make its way into the scintillator volume. Delaying this travel of radon long enough for it to decay before reaching the scintillator is in fact the primary purpose of the nylon vessels.

$^{218}\text{Po}$  is the last  $\alpha$  emitter in the row. As it has a half-life of only 3.1 minutes, it may well be possible to tag the successive decays of radon, this isotope, and the following

three. Their half-lives are short enough to guarantee that all are in secular equilibrium together. Section 8.4 provides a detailed discussion of this possibility.

$^{214}\text{Pb}$  is an undistinguished  $\beta^-$  emitter which frequently produces  $\gamma$  rays during its decay.

The most common are emitted at 351 and 295 keV;  $\gamma$  energies up to 839 keV are (rarely) possible.

$^{214}\text{Bi}$  ( $\beta^-$ ) and  $^{214}\text{Po}$  ( $\alpha$ ) are usually easily detected due to the very short lifetime of the latter isotope. However, atoms of  $^{214}\text{Bi}$  located outside the scintillator may produce high-energy  $\gamma$  rays that travel into the scintillator or even Fiducial Volume. The most common have energies of 609 keV, 1.76 MeV and 1.12 MeV. Energies up to 2.15 MeV may occur.

$^{210}\text{Pb}$  is essentially undetectable due to its low Q-value of 63 keV. However, its long half-life (22 years) gives it ample time to travel into the detector and produce progeny. Some studies have been performed (refer to Section 4.4.4, for instance) on its affinity for sticking to various surfaces and then washing off into scintillator that passes over those surfaces.

$^{210}\text{Bi}$  is a pure  $\beta^-$  emitter with a Q-value of 1.16 MeV, putting many of its decays in the neutrino energy window.

$^{210}\text{Po}$  is an  $\alpha$  emitter and the final radioisotope in the uranium series. Like  $^{210}\text{Pb}$ , it has some affinity for adhering to surfaces.

To summarize, the major concerns in this decay chain with respect to scintillator contaminants are the pure  $\beta^-$  emitters  $^{234\text{m}}\text{Pa}$  and  $^{210}\text{Bi}$ . Although each isotope will be in secular equilibrium with its parent, the parent is either indistinguishable from  $^{14}\text{C}$  background (in the former case) or nearly invisible to Borexino (in the latter case). The  $\alpha$  emitter  $^{210}\text{Po}$  is also a concern, just because it may be a large background as a result of “wash-off” of  $^{210}\text{Pb}$  and  $^{210}\text{Po}$  atoms from metal surfaces over which the scintillator passes. Finally, atoms of

| Species                 | Decay mode | Q value [MeV] | $E_\alpha$ or $E_{\beta+\nu}$ [MeV] | $E_\gamma$ [MeV] | Branching ratio [%] | Half-life $\tau_{1/2}$ |
|-------------------------|------------|---------------|-------------------------------------|------------------|---------------------|------------------------|
| $^{232}\text{Th}$       | $\alpha$   | 4.081         | 4.011                               | -                | 77                  | 14.1 Gyr               |
| $^{228}\text{Ra}$       | $\beta^-$  | 0.046         | 0.039                               | 0.007            | 60                  | 5.76 yr                |
| $^{228}\text{Ac}$       | $\beta^-$  | 2.137         | 1.11                                | 1.03             | 53                  | 6.13 h                 |
| $^{228}\text{Th}$       | $\alpha$   | 5.520         | 5.423                               | -                | 72.7                | 1.91 yr                |
| $^{224}\text{Ra}$       | $\alpha$   | 5.789         | 5.686                               | -                | 95.1                | 3.66 d                 |
| $^{220}\text{Rn}$       | $\alpha$   | 6.405         | 6.288                               | -                | 99.9                | 55.6 s                 |
| $^{216}\text{Po}$       | $\alpha$   | 6.907         | 6.779                               | -                | $\sim 100$          | 145 ms                 |
| $^{212}\text{Pb}$       | $\beta^-$  | 0.573         | 0.334                               | 0.239            | 83                  | 10.6 h                 |
| $^{212}\text{Bi}$ (64%) | $\beta^-$  | 2.246         | 2.246                               | -                | 55                  | 60.6 m                 |
| $^{212}\text{Po}$       | $\alpha$   | 8.954         | 8.784                               | -                | $\sim 100$          | 299 ns                 |
| $^{212}\text{Bi}$ (36%) | $\alpha$   | 6.207         | 6.051                               | 0.040            | 25                  | 60.6 m                 |
| $^{208}\text{Tl}$       | $\beta^-$  | 4.992         | 1.794                               | 3.198            | 51                  | 3.05 m                 |
| $^{208}\text{Pb}$       | stable     |               |                                     |                  |                     |                        |

Table 2.4: Summary table of the Thorium-232 decay chain.

$^{214}\text{Pb}$  and  $^{214}\text{Bi}$  outside the inner nylon vessel may emit high-energy  $\gamma$  rays that travel all the way into the Fiducial Volume. All of these problems must be guarded against.

The maximum level of uranium contamination considered acceptable in the Borexino scintillator is about  $10^{-16}$  g/g. Under the assumption of secular equilibrium, this contamination level would lead to an event rate of  $\sim 100$  events/day in the Fiducial Volume and  $^7\text{Be}$  neutrino energy window [12], but most ( $\sim 90$ ) of these would be easily identified  $\alpha$  decays.

### The thorium series

Isotopes in the thorium series are described below. Refer to Figure 2.4 or Table 2.4 for their decay energies and half-lives.

$^{232}\text{Th}$ , an  $\alpha$ -emitter, is the progenitor of the chain. It is present in typical rock dust at 10.3 ppm by weight, resulting in an activity of 41 mBq/kg [62]. This activity must be multiplied by a factor of ten when accounting for all the other isotopes in the series.

$^{228}\text{Ra}$  is unimportant in Borexino, with a Q-value of only 46 keV.

$^{228}\text{Ac}$  emits a  $\beta^-$  with a Q-value of 2.14 MeV. This isotope produces a complex  $\gamma$  spectrum, including  $\gamma$  rays at energies 911, 969, and 338 keV.  $\gamma$  ray levels up to about 2 MeV may occur.

$^{228}\text{Th}$  and daughters  $^{224}\text{Ra}$ ,  $^{220}\text{Rn}$ , and  $^{216}\text{Po}$  are  $\alpha$  emitters. The last three of these may be tagged as a “triple- $\alpha$  coincidence” given the short half-lives of  $^{220}\text{Rn}$  and  $^{216}\text{Po}$ .

$^{212}\text{Pb}$  is a  $\beta^-$  emitter with an end-point at 573 keV, in the neutrino window. It may produce  $\gamma$  rays, the most common at 239 keV.

$^{212}\text{Bi}$  may decay either by  $\alpha$  (36%) or  $\beta^-$  (64%). A  $\beta$  decay is easily seen because it is immediately followed by the  $\alpha$  decay of the extremely short-lived  $^{212}\text{Po}$ . In this case it may conceivably be possible to identify the  $^{212}\text{Pb}$  event between this coincidence and the preceding triple- $\alpha$  coincidence.

$^{208}\text{Tl}$  is on the lower-probability decay branch from  $^{212}\text{Bi}$ . It has a high-energy  $\beta^-$  decay that always releases a 2.615 MeV  $\gamma$  ray; 99.97% of the time, at least one additional  $\gamma$  ray with a minimum energy of 0.583 MeV is also produced. When it occurs within the scintillator, this high-energy decay and relatively short (3.1 minute) half-life may be sufficient to identify the  $^{212}\text{Bi}/^{208}\text{Tl}$  pair of decays. However, the penetrating  $\gamma$  rays make it the most dangerous isotope in either decay chain for detector components outside the inner nylon vessel. The exact rate of  $^{208}\text{Tl}$  events may be crucial in determining whether or not it will be possible for Borexino to observe *pep* neutrinos.

Within the thorium series, potentially troublesome isotopes within the scintillator volume include the  $\beta^-$  emitters  $^{228}\text{Ac}$  and  $^{212}\text{Pb}$ . Most other isotopes in the series will be identifiable either as  $\alpha$  decays through  $\alpha/\beta$  discrimination, or through the method of coincidences (in some cases, extended over several minutes). The most difficult challenge, however, will be the penetrating high-energy  $\gamma$  rays produced by  $^{208}\text{Tl}$  atoms embedded in the photomultipliers and other pieces of detector hardware.

The maximum level of thorium contamination considered acceptable in the Borexino scintillator is about  $10^{-16}$  g/g. Under the assumption of secular equilibrium, this contamination level would lead to an event rate of about 23 events/day in the Fiducial Volume and  ${}^7\text{Be}$  neutrino energy window [12]. About 19 of these events would be easily detectable  $\alpha$  decays.

#### 2.2.4 Categories of radioactive background

The isotopes described in this section, and possibly others that have not yet been considered, contribute to three types of radioactive background in the detector, based upon the location of the decaying nuclides.

Internal background consists of the decays of radioactive atoms that happen to be impurities in the scintillator fluid or that are generated cosmogenically by interactions of muons with the scintillator. These decays will most probably occur with a homogeneous distribution throughout the scintillator volume. Some internal background rates, such as that due to  ${}^{39}\text{Ar}$ , are predictable since the background comes entirely from materials (the LAK  $\text{N}_2$ ) with known concentrations of radioisotopes. Some background rates, such as those of the cosmogenic isotopes, are predictable because they depend only upon measured physical quantities such as muon interaction cross-sections and the muon flux at the depth of Borexino. Other background rates, such as that of  ${}^{40}\text{K}$ , are not really predictable. The numbers of atoms of these species found in the scintillator depend upon both the scintillator's initial level of contamination and upon the effectiveness of purification methods at removing contaminants. Neither are really known *a priori*. For this reason, estimating the total expected background rate in Borexino before the detector begins data acquisition would be a fairly meaningless exercise, though the rates resulting from certain individual species may be calculated with reasonable confidence.

Attempts to measure the rates of these isotopes with the 4-ton Borexino prototype, the Counting Test Facility (CTF), have been inconclusive for two reasons. First, the history

of the CTF has been complex. Numerous purification tests have been performed on its scintillator, making it unclear whether the presence of certain contaminants at a given moment results from an inadequacy in the most recent purification method, or from their introduction into the scintillator by accident during a previous test. Some contaminants (the mass-210 isotopes, for instance) are known to adhere readily to various nylon and metal surfaces, and later “wash off” back into purified scintillator. Second, as the CTF has a mass of only  $\frac{1}{25}$  that of the Borexino Fiducial Volume, the inability to detect a certain isotope in the CTF says nothing about whether it will be a problem for Borexino.

Despite these facts, the CTF is a most invaluable tool. Though it can never conclusively say that a certain isotope will not cause trouble for the Borexino detector, it *can* point out the most problematic areas. It has been used to test materials to be used in Borexino, scintillator purification techniques, and perform the most sensitive measurement ever made of the  $^{14}\text{C}$  levels in petroleum derivatives. The CTF is described in great detail in Chapter 6, and the following chapters discuss results for internal contamination that *can* unequivocally be concluded from CTF data.

A second type of background in Borexino may be classified as surface background. This background is caused by radioactive atoms either adsorbed on the inner surface of the nylon vessel that contains the scintillator, or embedded within it. Those atoms sufficiently close to the inner surface of the nylon film can release an  $\alpha$  or  $\beta$  particle into the scintillator. Any decay in the nylon may produce a  $\gamma$  ray that travels inward, to be observed as an event. Radium atoms in the nylon will continually decay into radon, which may migrate into the scintillator and itself decay there. This process is called emanation. Finally, radon atoms from outside the inner nylon vessel may even travel all the way through it, eventually to end up in the Fiducial Volume. These possibilities are all discussed in relation to the Borexino nylon vessels in Section 4.4. Investigations of surface background in the CTF are performed in Chapter 9.

Finally, one of the most difficult types of background to deal with is the external background caused by high-energy  $\gamma$  rays produced outside the inner nylon vessel, which nevertheless travel all the way into the volume of scintillator. The specific activities for various detector components are known fairly well, for instance in [63]. However, they produce a continuous energy spectrum in the scintillator whose precise shape and amplitude is difficult to predict, even with Monte Carlo methods. The presence of a  $\gamma$ -ray continuum has posed serious difficulties for analyses of internal contaminant concentrations based upon the observed energy spectrum of the CTF. Some discussion on the problem in the CTF is given in Section 9.4 of this work. Monte Carlo simulations of the expected Borexino external background are presented in, for instance, [12, 48, 49].

### 2.3 Prospects for observing solar neutrinos

The solar neutrino signal that can be measured in Borexino will depend upon the target mass and lifetime of the detector; the flux of neutrinos at Earth; the cross-section for each neutrino flavor to react in a visible way; and the fraction of surviving electron neutrinos. The latter three of these are functions of the incident neutrino energies. We will assume a detector lifetime of 10 years. The flux of neutrinos at Earth is given essentially by their rate of production in the Sun, which was discussed in Section 1.3.

As already mentioned, the means of observing solar neutrinos in Borexino is through elastic scattering on electrons,  $\nu + e^- \rightarrow \nu + e^-$ . (Neutrino capture by a  $^{12}\text{C}$  nucleus,  $^{12}\text{C} + \nu_e \rightarrow ^{12}\text{N} + e^-$ , cannot occur unless the neutrino energy is greater than 17 MeV. The threshold for capture by  $^{13}\text{C}$  is only 2.2 MeV, but the isotopic abundance of  $^{13}\text{C}$  is fairly low, 1.1%.) Given a certain incident energy  $E_\nu$  for the neutrino, the kinetic energy spectrum of the electron is uniquely determined by the differential cross-section for the interaction. When the electron is scattered in the direction in which the neutrino was initially traveling, it is imparted the maximum kinetic energy possible for a given neutrino energy. This kinetic



Figure 2.5: First-order Feynman diagrams for neutrino-electron elastic scattering. All neutrinos may scatter on electrons via a neutral-current interaction involving the exchange of a virtual  $Z^0$  (left). Only electron neutrinos may scatter on electrons by the mediation of a charged virtual  $W$  particle (right).

energy is given by classical kinematic arguments as

$$E_{\max} = \frac{E_\nu}{1 + m_e c^2 / (2E_\nu)}. \quad (2.13)$$

### 2.3.1 The ${}^7\text{Be}$ neutrinos

The 862 keV  ${}^7\text{Be}$  solar neutrinos will be observed in Borexino as an electron recoil spectrum that is nearly constant up to an energy of 667 keV, at which point it descends sharply to zero. This feature, the Compton edge, will in practice be smeared by the finite energy resolution of the detector. (Because the electron capture decay of  ${}^7\text{Be}$  has a 10.4% branching ratio to an excited state of  ${}^7\text{Li}$ , a fraction of  ${}^7\text{Be}$  neutrinos are produced with an energy of 384 keV, implying a second Compton edge at 230 keV. This signal will be obscured by  ${}^{14}\text{C}$  background. Below we consider only the 862 keV  ${}^7\text{Be}$  neutrinos.)

Below the maximum recoil energy, the differential cross section for a given neutrino energy  $E_\nu$  is given by

$$\frac{d\sigma}{dE}(E; E_\nu) = \frac{\sigma_0}{m_e c^2} \left[ g_\ell^2 + g_r^2 \left(1 - \frac{E}{E_\nu}\right)^2 - g_\ell g_r \frac{m_e c^2 E}{E_\nu^2} \right], \quad (2.14)$$

where  $\sigma_0 \equiv 2G_F^2 m_e^2 / (\pi \hbar^4) = 8.81 \times 10^{-45} \text{ cm}^2$ . The value  $g_r = \sin^2 \theta_w \approx 0.222$  for all neutrinos. The value  $g_\ell$  is  $\sin^2 \theta_w + 1/2 \approx 0.722$  for electron neutrinos, and  $\sin^2 \theta_w - 1/2 \approx -0.278$  for other neutrino flavors. The difference comes from the ability of electron neutrinos

to scatter from electrons by a charged-current reaction, whereas other neutrinos can scatter from electrons only via a neutral current (Figure 2.5). The angle  $\theta_w$  itself is the weak mixing angle.

The total cross section for a neutrino of energy  $E_\nu$  is simply the integral of this expression from  $E = 0$  up to  $E_{\max}$ :

$$\sigma(E_\nu) = \sigma_0 \frac{E_{\max}}{m_e c^2} \left[ (g_\ell^2 + g_r^2) - \left( \frac{g_r^2}{E_\nu} + g_\ell g_r \frac{m_e c^2}{2E_\nu^2} \right) E_{\max} + g_r^2 \frac{E_{\max}^2}{3E_\nu^2} \right]. \quad (2.15)$$

Suppose that the flavor composition of the neutrino beam is known: a fraction  $P_e$  of the beam consists of electron neutrinos. Then we may define effective differential and total cross sections by replacing  $g_\ell$  and  $g_\ell^2$  in Equations (2.14) and (2.15) by their average values:

$$\langle g_\ell \rangle = \sin^2 \theta_w - 1/2 + P_e \approx P_e - 0.278 \quad (2.16)$$

$$\langle g_\ell^2 \rangle = \sin^4 \theta_w - \sin^2 \theta_w + 1/4 + 2P_e \sin^2 \theta_w \approx 0.444 P_e + 0.0773. \quad (2.17)$$

For the 862 keV  ${}^7\text{Be}$  neutrinos, Equation (2.15) yields  $\sigma_e = 0.659 \sigma_0$  for electron neutrinos ( $P_e = 1$ ), and  $\sigma_{\mu,\tau} = 0.147 \sigma_0$  for  $\mu$ - or  $\tau$ -neutrinos ( $P_e = 0$ ). In the limit  $E_\nu \gg m_e c^2$ , the respective results become  $\sigma_e \rightarrow 0.538 \sigma_0 (E_\nu / m_e c^2)$  and  $\sigma_{\mu,\tau} \rightarrow 0.094 \sigma_0 (E_\nu / m_e c^2)$ .

With a monoenergetic neutrino beam of energy  $E_\nu$ , the number of interactions observed to yield electron kinetic energies in a specified narrow range  $[E, E + dE]$  is given by the energy width  $dE$  multiplied by the incident neutrino flux  $\Phi$ , the differential cross-section  $d\sigma/dE$  (weighted appropriately for electron neutrinos and other flavors), number density of electrons in the target  $n$ , volume  $V$  of the target, and time  $T$  for which it is observed. That is:

$$\frac{dN}{dE} dE = nVT \Phi \frac{d\sigma_{\text{eff}}}{dE} dE. \quad (2.18)$$

This can be rewritten as  $nVT \Phi \sigma_{\text{eff}} \rho_r(E; E_\nu)$ . Here,  $\rho_r(E; E_\nu) \equiv (1/\sigma_{\text{eff}}) (d\sigma_{\text{eff}}/dE)$  is the normalized (integral = 1) electron kinetic energy spectrum of the interaction.

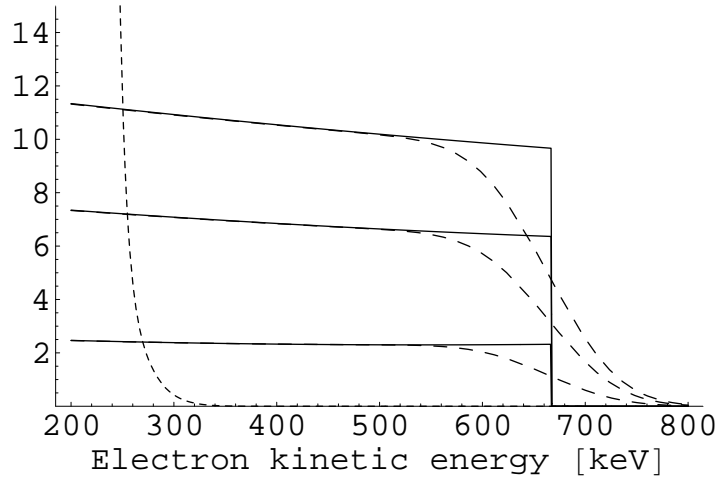


Figure 2.6: The spectrum of electrons scattered by  ${}^7\text{Be}$  neutrinos that should be observed in Borexino, given the two extreme cases of (top curve) no neutrino oscillations; (bottom curve) complete oscillation into  $\mu$ - and  $\tau$ -neutrinos. The middle curve shows the expected result when  $P_e = 0.55$  as predicted for energies where the MSW effect does not contribute much and vacuum oscillations dominate. Values on the  $y$ -axis are given in units of events per day per 100 keV. Solid lines are the ideal theoretical spectra, with a sharp Compton edge at 667 keV. Dashed lines represent smearing effects due to finite energy resolution. The steeply descending dotted curve that falls to zero near 300 keV indicates the expected  ${}^{14}\text{C}$  background (both individual and “pile-up” events).

The observed kinetic energy spectrum  $\rho_d$  will be the convolution of the true spectrum  $\rho_r$  with the energy resolution function, as described previously in Section 2.1. Hence, the total rate of  ${}^7\text{Be}$  neutrinos observed in the Borexino Fiducial Volume with energies greater than 250 keV will be  $nV\sigma_{\text{eff}} \int_{250\text{ keV}}^{\infty} \rho_d(E; E_\nu) dE$ . (Below 250 keV,  ${}^{14}\text{C}$  background will dominate, hiding the neutrino signal.) To simplify the calculation,  $\rho_d$  in this integral may be replaced by  $\rho_r$  with little error, as the function  $d\sigma_{\text{eff}}/dE$  is fairly flat over most of its range (Figure 2.6).

In the case of Borexino,  $nV = 3.31 \times 10^{31}$  electrons in the Fiducial Volume. The flux of 862 keV  ${}^7\text{Be}$  neutrinos at Earth is  $89.6\% \times 4.84 \times 10^9 \text{ cm}^{-2}\text{s}^{-1}$  [5, 10]. (The estimated error in this figure, due to uncertainties in the Standard Solar Model, is a relatively high 10.5%.) If no neutrino oscillations occurred, the rate of  ${}^7\text{Be}$  neutrinos observed in the Fiducial Volume

with  $E > 250$  keV would be 43 per day. If, on the other hand, *all* neutrinos were converted to  $\mu$  and  $\tau$  flavors during their travels, the expected rate of  ${}^7\text{Be}$  neutrinos above 250 keV would become only 10 per day. The expected value of  $P_e$  is about 0.55, a result obtained from the prediction (as discussed in the previous chapter) that the MSW effect is small for  ${}^7\text{Be}$  neutrinos even at the densities found in the Sun's core. For  $P_e = 0.55$ , the expected  ${}^7\text{Be}$  neutrino event rate is 28 per day at energies above 250 keV. (Taking into account the *pep* and CNO neutrino signals described below in Section 2.3.3 will add roughly four additional events per day in the 250–800 keV range to this figure.) These numbers indicate that the actual observed neutrino event rate will be a sensitive indicator of the probability of neutrino oscillation.

In the best possible case (no non-removable background), assuming the value of  $P_e$  given above, a total of about  $10^5$   ${}^7\text{Be}$  neutrinos would be observed in events over the 250 keV threshold during ten years of detector operation. The statistical error in the calculated neutrino flux would be 0.3%. Of course, this situation cannot be achieved, and the real question for the detector sensitivity is what level of background noise may be attained. One may consider several types of background. The most harmless is that which may be “tagged” and excluded from the data sample *a priori*, for instance the  ${}^{214}\text{BiPo}$  and  ${}^{212}\text{BiPo}$  coincidence events caused by the very short half-lives of those two polonium isotopes.  $\alpha/\beta$  discrimination, removing 90–95% of  $\alpha$  events from the data sample, is a second example of event tagging. Of the remaining background, some of it may be assumed to have a known rate because it is in secular equilibrium with taggable events. This is the case, for instance, with  ${}^{212}\text{Pb}$  in the thorium chain. Other backgrounds ( ${}^{40}\text{K}$ ,  ${}^{85}\text{Kr}$ , etc.) have imprecisely known rates but accurately known spectral shapes. The most troublesome backgrounds are those which exhibit neither, for instance external  $\gamma$  rays whose spectrum can be at best simulated with Monte Carlo methods.

Consider the case where the background spectrum is known perfectly, so it can be statistically subtracted from the neutrino signal. We suppose that events which can be individually tagged have already been purged from the data. Let the total number of events observed in

the neutrino window be  $N_t$ , of which  $N_s$  are the neutrino signal and  $N_b$  are well-understood background. Hence  $N_s = N_t - N_b$ . Propagating the errors, we find

$$\begin{aligned}\delta N_s &= \sqrt{\delta N_t^2 + \delta N_b^2} = \sqrt{N_t + N_b} = \sqrt{N_s + 2N_b} \\ &= \sqrt{N_s} \sqrt{1 + 2N_b/N_s}.\end{aligned}\tag{2.19}$$

That is, if the  $S/N$  ratio is 10, the statistical error in the result will be at least 10% greater than in the ideal case. If the  $S/N$  ratio is two—the known background rate is 50% of the neutrino rate—then the statistical error will be more than 40% greater. Most likely, in either case the systematic error (due to the existence of background with a poorly understood spectral shape) will be larger than the statistical error.

### 2.3.2 Annual variations in the ${}^7\text{Be}$ signal

Unfortunately there is no way to obtain an ideal measurement of the background rate in Borexino. The solar neutrino signal cannot be turned off to disentangle it from the background. It can, however, be varied—slightly. The Earth has an orbit with an eccentricity  $\epsilon \approx 0.0167$  and semi-major axis  $a \approx 1.496 \times 10^8$  km. The distance between the center and a focus of an ellipse is  $\epsilon a$ . At aphelion, in July, the Earth-Sun distance is 3.4% greater than at perihelion, in January. Flux received from the Sun varies as the inverse square of the distance: the maximum neutrino flux is 6.9% higher than the minimum flux.

This fact will permit us to measure the solar neutrino flux without potential ambiguities due to background with poorly known spectral shapes. Suppose that the background in the neutrino window 250–800 keV has rate  $B$ , and that the average neutrino signal has rate  $S_0$ . In January, we have a signal of rate  $(1+2\epsilon)S_0$ , and in July, neutrino rate  $(1-2\epsilon)S_0$ . The total signal over  $n$  Januaries (each of length  $T = 31$  days) becomes  $N_{\max} = nT[B + (1 + 2\epsilon)S_0]$ , and over  $n$  months of July becomes  $N_{\min} = nT[B + (1 - 2\epsilon)S_0]$ , with respective statistical errors given by the square roots of those values. The difference is then  $N_{\max} - N_{\min} =$

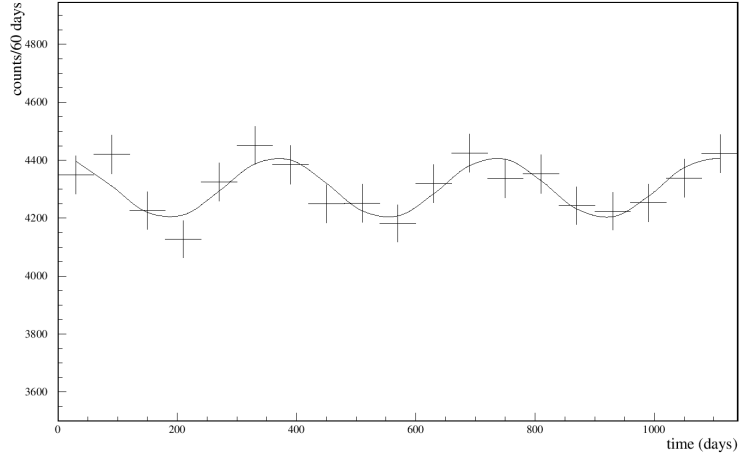


Figure 2.7: Simulated data, showing the accumulated neutrino signals over one-month periods for three years as a function of time. This figure illustrates the expected annual variation in the neutrino flux due to the eccentricity of the Earth's orbit. Though this simulation was performed assuming no oscillations, the actual expected data should be similar, although with only about 65% of the numbers of events shown. Figure taken from reference [64].

$4\epsilon nTS_0 \pm \sqrt{2nT(S_0 + B)}$ . The statistical error as a fraction of the difference is

$$\frac{\delta(\Delta N)}{\Delta N} \equiv \frac{\delta S_0}{S_0} = \frac{\sqrt{2}}{4\epsilon} \frac{1}{\sqrt{nTS_0}} \sqrt{1 + \frac{B}{S_0}}. \quad (2.20)$$

Plugging in the numbers, assuming  $S_0 = 28$  events/day and  $n = 10$  (years), we obtain  $\delta S_0/S_0 \approx 0.23\sqrt{1 + B/S_0}$ . Though a 20% statistical error is quite large in comparison with the error quoted earlier (due to the small value of  $\epsilon$  and the much reduced period of data collection), it must be noted that the value obtained in this way will include no systematic error due to background spectral shapes. It may also be reduced further by including other months in the data sample and fitting a periodic function to the results,

$$S(t) = S_0 \left[ 1 + 2\epsilon \cos\left(\frac{2\pi t}{1 \text{ yr}}\right) + O(\epsilon^2) \right], \quad (2.21)$$

as shown in Figure 2.7.

Observation of the neutrino flux variation as a function of time is not only useful as a cross-check for systematic errors caused by background. It may also point to new physics if the

observed variation does not match the expected value of  $\sim 7\%$ . Such unexpected annual variations might indicate that, contrary to theory, the  ${}^7\text{Be}$  neutrino oscillates in vacuum over length scales on the order of  $2\epsilon a \approx 5 \times 10^6$  km.

### 2.3.3 The *pep* and CNO cycle neutrinos

Borexino may have the ability to observe the *pep* solar neutrinos, and (depending upon their rate of production in the Sun) also the CNO cycle neutrinos, in the energy range 0.8–1.3 MeV. The *pep* neutrinos are produced at the single energy 1.44 MeV, implying a Compton edge at 1.22 MeV. Their expected flux at Earth is  $\Phi_{pep} = 1.42 \times 10^8 \text{ cm}^{-2}\text{s}^{-1}$ , with an uncertainty of only 2% [5, 10].

Unlike the  ${}^7\text{Be}$  and *pep* neutrinos, those produced in the CNO cycle originate in the  $\beta^+$  decays of the species  ${}^{13}\text{N}$ ,  ${}^{15}\text{O}$ , and  ${}^{17}\text{F}$ . The CNO neutrinos therefore have continuous spectra that range from zero to the Q-values of these decays (less  $2m_e c^2$ , to account for positron annihilation). Their spectra are given by Equation (2.8) with the substitution  $E \rightarrow Q - 2m_e c^2 - E_\nu$ ; that is, they are mirror images of the positron kinetic energy spectra.

The respective end points of the  ${}^{13}\text{N}$ ,  ${}^{15}\text{O}$ , and  ${}^{17}\text{F}$  neutrino spectra are at 1.20, 1.73, and 1.74 MeV, giving end points for the recoil electron spectra at 0.99 and 1.51 MeV. The predicted fluxes of these species in the 2005 SSM are roughly  $\Phi_{13\text{N}} = 3.05 \times 10^8$ ,  $\Phi_{15\text{O}} = 2.31 \times 10^8$ , and  $\Phi_{17\text{F}} = 5.83 \times 10^6 \text{ cm}^{-2}\text{s}^{-1}$  [5, 10]. (Hence the  ${}^{17}\text{F}$  neutrino will be essentially impossible to observe separately from the  ${}^{15}\text{O}$  neutrino; it will have the effect of increasing the observed  ${}^{15}\text{O}$  signal by about 2.5%.) It should be noted that these estimates for the  ${}^{13}\text{N}$  and  ${}^{15}\text{O}$  fluxes are about half those in the 2004 SSM due to a newly measured value for the cross section of the fusion reaction  ${}^{14}\text{N}(p, \gamma){}^{15}\text{O}$ . The estimated errors in the values are also large (30%+) due mainly to uncertainties in the solar composition for heavy element abundances [5]. A measurement of the CNO neutrino flux would therefore be invaluable in improving the accuracy of the SSM.

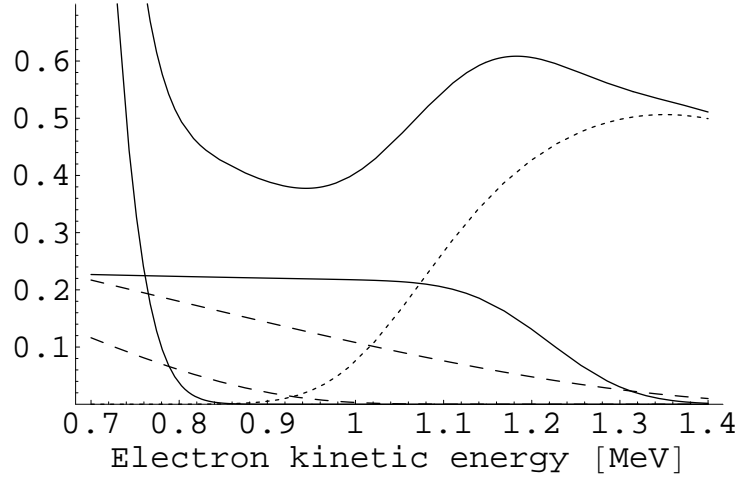


Figure 2.8: Expected spectrum of solar neutrino events in the 100-ton Fiducial Volume, in events per day per 0.1 MeV, for the energy range 0.7–1.4 MeV. The edge at about 750 keV is the tail of the  ${}^7\text{Be}$  neutrino distribution. Note that the vertical scale is much enlarged from Figure 2.6! The two dashed curves represent (upper) the  ${}^{15}\text{O}$  and (lower)  ${}^{13}\text{N}$  neutrinos from the CNO cycle; their amplitudes are uncertain by roughly 30%. The mainly horizontal solid curve, coming to an end near 1.35 MeV, is the  $pep$  neutrino spectrum. The dotted curve that peaks near 1.4 MeV is the  ${}^{11}\text{C}$  radioactive background, suppressed by about a factor of five with delayed coincidence time and radial cuts. The uppermost curve is the expected total of all these signals.

For a neutrino with a continuous spectrum, Equation (2.18) and the definition of the electron kinetic energy spectrum  $\rho_r(E; E_\nu) \equiv (1/\sigma_{\text{eff}}) (d\sigma_{\text{eff}}/dE)$  must be generalized to integrals over the normalized energy spectrum  $\rho_\nu$  of the neutrino:

$$\frac{dN}{dE} = nVT \Phi \int_0^\infty \frac{d\sigma_{\text{eff}}}{dE}(E; E_\nu) \rho_\nu(E_\nu) dE_\nu \quad (2.22)$$

$$\rho_r(E) = \int_0^\infty \rho_r(E; E_\nu) \rho_\nu(E_\nu) dE_\nu = \frac{\int_0^\infty (d\sigma_{\text{eff}}/dE) \rho_\nu(E_\nu) dE_\nu}{\int_0^\infty \sigma_{\text{eff}}(E_\nu) \rho_\nu(E_\nu) dE_\nu}. \quad (2.23)$$

In principle the differential and total cross sections within the integrals depend upon the neutrino energy, both directly through  $E_\nu$  and  $E_{\text{max}}$  as shown in Equations (2.14) and (2.15), and indirectly through the energy dependence of  $P_e$ , the survival probability  $P(\nu_e \rightarrow \nu_e | E_\nu)$  for neutrinos traveling to meet us from the core of the Sun. However, in this energy regime

$P_e$  is still rather less than the vacuum-matter transition energy around 2 MeV. It is therefore predicted to be only weakly energy-dependent in this range, and may be approximated as  $\sim 0.55$ .

These considerations permit us to conclude that, within the 100-ton Fiducial Volume, the rate of *pep* neutrinos in the 0.8–1.3 MeV energy range will be 0.9 per day. That of the  $^{13}\text{N}$  and  $^{15}\text{O}$  neutrinos (combined) in this range will be 0.5 per day. The rate of  $^{11}\text{C}$  radioactive background in this range, however, will be about 1 event/day, even if 80% of the  $^{11}\text{C}$  background is suppressed by the delayed coincidence time and radial cuts described earlier. Figure 2.8 shows the expected energy spectrum in this range.

Let us assume a total data-taking time of 10 years. The  $^{11}\text{C}$  exclusion cuts will reduce this figure by 7% to 9.3 years, giving total expected values for  $N_s \approx 5000$  neutrino events in the 0.8–1.3 MeV range, and for a  $^{11}\text{C}$  background in the same energy window of  $N_b \approx 3500$  events. From Equation (2.19), the statistical error in the measured *pep*+CNO neutrino rate will be about 2%. If we also treat the *pep* neutrinos as “background” in order to get a measurement of the CNO cycle neutrinos, we will see roughly 1700 CNO neutrinos with a statistical error of about 7%. This will still provide a significantly better estimate than the current uncertainties in the CNO rates of 30%.

It should be noted that, due to external background from the PMTs and other sources, the Fiducial Volume for *pep* neutrino analysis may have to be reduced to only 70 tons of scintillator. In this case, the statistical errors quoted in the preceding paragraph must all be multiplied by a factor of 1.7. It should also be noted that we have made no methodical consideration of potential systematic errors from background other than  $^{11}\text{C}$  in the *pep*/CNO neutrino energy window.

## 2.4 Prospects for observing other neutrinos

### 2.4.1 Geoneutrinos and reactor antineutrinos

Borexino may observe antineutrinos from two sources. The first is the radioactive decay of elements in the Earth's crust and mantle. Each radioactive decay by  $\beta^-$  emission produces an electron antineutrino. The second source of antineutrinos consists of nuclear reactors in Europe, within a few hundred km of the detector. Just as with solar neutrinos, low-energy antineutrinos may in principle be detected via electron scattering:

$$\bar{\nu} + e^- \rightarrow \bar{\nu} + e^- \quad (2.24)$$

However, any antineutrino signal in the sub-MeV range is expected to be swamped by the  ${}^7\text{Be}$  solar neutrinos, particularly since the cross section for  $\bar{\nu}_e e^-$  scattering is much smaller over most of this energy range than for  $\nu_e e^-$  scattering.

A distinctive signal for antineutrinos with sufficiently high energies is available through the inverse  $\beta$ -decay reaction on protons,

$$\bar{\nu}_e + p \rightarrow n + e^+. \quad (2.25)$$

The reaction can occur only for electron antineutrinos. The minimum antineutrino energy required for the reaction is  $(m_n + m_e - m_p)c^2 \approx 1.8 \text{ MeV}$ . Since most of the kinetic energy is carried away by the positron, the spectrum is nearly monoenergetic given a specific antineutrino energy. The immediately following annihilation of the positron means that the energy observed for the reaction is  $E \approx E_\nu - 782 \text{ keV}$ . Thus, the observed energy is always greater than  $2m_e c^2$ .

By itself, this fact would be insufficient to detect the antineutrino signal; many radioactive backgrounds may be present in this energy range. However, the neutron travels less than a meter before being captured by another proton, forming a deuterium nucleus. In the process a  $2.2 \text{ MeV}$   $\gamma$  ray is emitted. The mean time until capture is about  $250 \mu\text{s}$  [41]. The

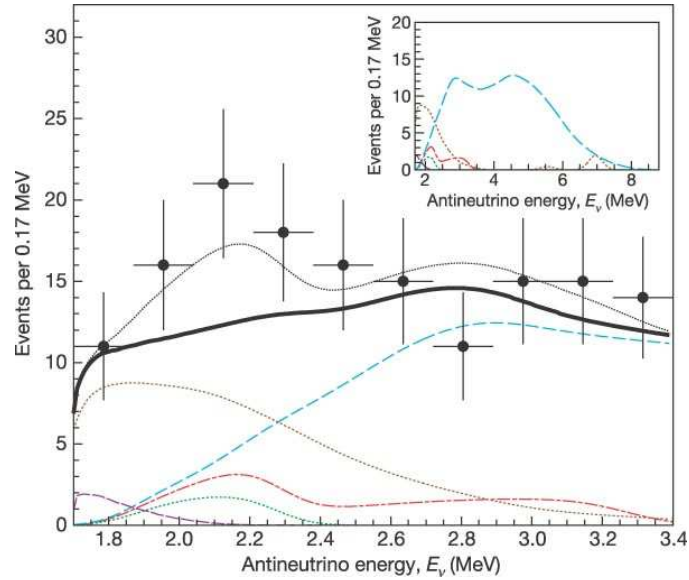


Figure 2.9: The antineutrino signals observed by the KamLAND detector. The points are the experimentally observed values for 0.17 MeV-wide bins, shown with  $1\sigma$  vertical bars. Total expected signal is given by the thin dotted black line. The solid bold line is the theoretical sum of all backgrounds. Individual backgrounds shown include reactor antineutrinos (blue dashed curve), the reaction  $^{13}\text{C}(\alpha, n)^{16}\text{O}$  (yellow dotted curve), and accidental coincidences (low-amplitude violet dashed curve at far lower left). Signals include the  $^{238}\text{U}$  chain antineutrinos (dot-dashed red curve) and  $^{232}\text{Th}$  chain antineutrinos (dotted green curve). Figure taken from reference [65].

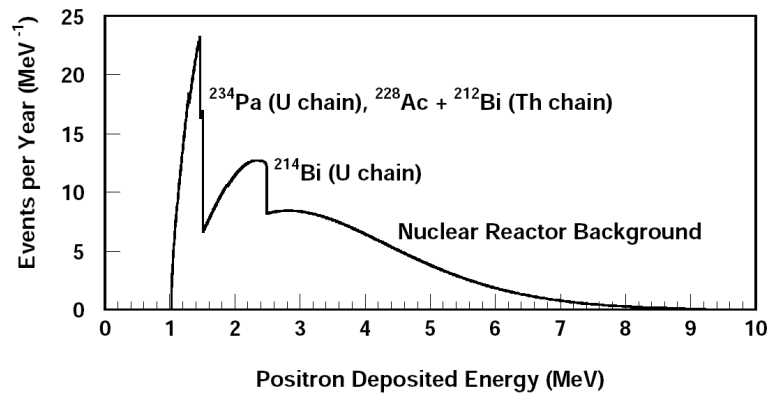


Figure 2.10: Predicted spectrum of antineutrinos from Earth-based radioactive decays and nearby nuclear reactors in Borexino. Figure taken from reference [51].

signal of an antineutrino event therefore consists of a coincidence with  $E_1 > 1.02 \text{ MeV}$  and  $E_2 \approx 2.2 \text{ MeV}$ . With appropriate radial and time cuts, background noise may be removed with high efficiency.

The rate of inverse  $\beta$  decay caused by geoneutrinos has been measured by the KamLAND experiment to be  $5.1_{-3.6}^{+3.9} \times 10^{-31} \bar{\nu}_e$  events per target proton per year [65]. In the 300 tons of scintillator in Borexino (there is no need to restrict analysis to the Fiducial Volume due to the high efficiency with which most background are excluded), containing  $1.35 \times 10^{31}$  hydrogen atoms, this corresponds to  $7 \pm 5$  events/yr. However, the rate will be rather different in various parts of the world, due to the varying radioactivity levels in continental and oceanic crust. Values of 10 events/yr (Figure 2.10) and 24 events/yr have been estimated for the specific location of Borexino in references [51, 52], respectively.

In KamLAND, the only significant background to interfere with detection of these antineutrinos (see Figure 2.9) is the reaction  $^{13}\text{C}(\alpha, n)^{16}\text{O}$ , caused when  $\alpha$  particles emitted by radon daughters collide with nuclei of  $^{13}\text{C}$  (present in normal carbon at 1% isotopic abundance). The number of such background events that passed the coincidence selection cuts, for KamLAND, was estimated at  $42 \pm 11$  over 749 days of live time in a spherical volume with 5-m radius [65]. The observed rate of  $^{210}\text{Po}$   $\alpha$ -decays (the main source of  $\alpha$  particles) in KamLAND was 33 Bq within a 5.5-m radius sphere [66]. Hence this reaction must produce an event rate of about  $2.5 \times 10^{-8}$  that of the  $\alpha$  decay rate in a detector.

For the Borexino  $S/N$  for geoneutrinos to exceed ten, we therefore require no more than  $7 \times 10^4$   $\alpha$  decays per day in the 300 tons of scintillator. Given that the target cleanliness level for Borexino is more on the order of  $< 90$   $\alpha$  decays per day in the central 100 tons, the detector should be able to fulfill this additional requirement automatically. Given that geoneutrinos should easily be seen in Borexino, reactor antineutrinos (which, as seen in Figures 2.9–2.10, extend up to 8 MeV in energy) also will certainly be detected. The expected signal due to European reactor power plants is about 28 per year, of which only about  $\frac{1}{4}$  will be below 3 MeV [51, 52].

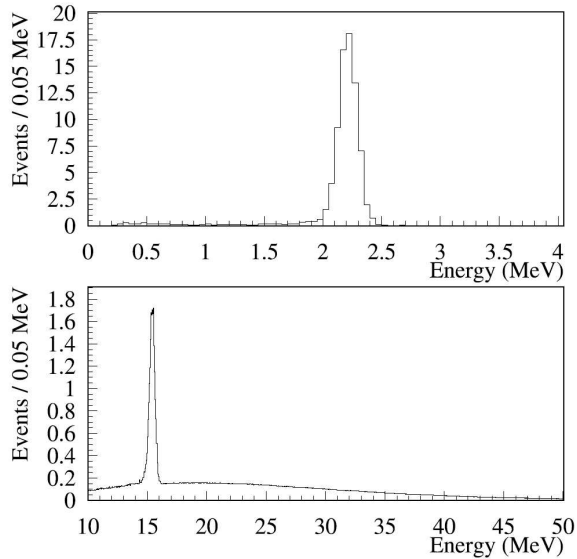


Figure 2.11: Simulated energy spectrum from supernova neutrinos in Borexino. In a low-energy window (top), many events will be due to the 2.2 MeV  $\gamma$  ray emitted during neutron capture after an inverse  $\beta$  decay reaction. ( $\nu p$  elastic scattering events were not included in this graph.) In the high-energy regime (bottom), there should be a prominent peak due to neutral-current reactions on  $^{12}\text{C}$  nuclei. The ability to tag  $\beta$  decays following charged-current  $^{12}\text{C}$  interactions should also make those events easily identifiable. Figure taken from reference [53].

### 2.4.2 Supernova neutrinos

If a supernova were to occur in or near our galaxy, Borexino would see a burst of events with a duration of about ten seconds. Several detection mechanisms are possible. The first is the simple neutrino-electron scattering that may occur for all flavors of neutrinos and antineutrinos (with electron neutrinos having the highest cross-section). Another is the just-discussed inverse beta decay, sensitive only to electron antineutrinos. Three reactions on  $^{12}\text{C}$  nuclei may also occur:

- The reaction  $^{12}\text{C}(\nu_e, e^-)^{12}\text{N}$  has a threshold of 17.3 MeV. The isotope  $^{12}\text{N}$  quickly decays again by  $\beta^+$  emission with a half-life of 11.0 ms.

- The reaction  $^{12}\text{C}(\bar{\nu}_e, e^+)^{12}\text{B}$  has a threshold of 14.4 MeV. The isotope  $^{12}\text{B}$  decays by  $\beta^-$  emission with a half-life of 20.2 ms.
- The reaction  $^{12}\text{C}(\nu_x, \nu_x)^{12}\text{C}^*$  (a neutral current inelastic scattering that promotes the  $^{12}\text{C}$  nucleus to an excited state  $J^\pi = 1^+$ ) has a threshold of 15.1 MeV. The excited state of  $^{12}\text{C}$  returns to the ground state immediately by emitting a monoenergetic 15.1 MeV  $\gamma$  ray. Since this is a neutral current reaction, any flavor of neutrino or antineutrino may be involved.

As described in reference [53], the total number of these events seen in the 300 tons of scintillator for a typical Type II supernova (total energy release of  $3 \times 10^{53}$  ergs) at a distance of 10 kpc should be approximately 110 (Figure 2.11). Of these,  $\sim 80$  should be inverse  $\beta$  decay reactions, indicating a  $\bar{\nu}_e$ . These will be easily recognizable because of the following 2.2 MeV  $\gamma$  ray produced by neutron capture on a proton. Another 4–5 will be charged-current reactions indicating  $\nu_e$ 's and  $\bar{\nu}_e$ 's; also easily identified by the following high-energy  $\beta^\pm$  decays. Of the remainder, about 22 will be neutral-current interactions with  $^{12}\text{C}$  (identifiable by the single monoenergetic 15.1 MeV  $\gamma$  ray), and about five will be electron scattering reactions; both channels are available to all flavors of neutrinos and antineutrinos. The great majority of these 110 events should be distinct and easily identifiable as supernova neutrino signals.

The inverse  $\beta$  decay and charged-current reactions with  $^{12}\text{C}$  are only relevant to  $\nu_e$  and  $\bar{\nu}_e$ . None of the neutral-current reactions described above really give an indication of the energy spectrum of the original neutrinos, so it is impossible from these data to determine the spectrum of  $\nu_{\mu,\tau}$  and  $\bar{\nu}_{\mu,\tau}$ . To remedy this deficiency, J. Beacom, W. Farr and P. Vogel proposed to look for neutral-current neutrino-*proton* scattering [54]. This process has a high-energy end point for the proton recoil kinetic energy at  $E_p \approx E_\nu^2/m_p c^2$ , and the differential cross section is weighted toward higher energies. However, as is the case with  $\alpha$  particles, the energy observed for protons moving in a liquid scintillator is heavily quenched; see for instance Section 3.1.2. The expected number of events resulting from  $\nu p$  scattering

above an observed energy threshold of 200 keV, for a standard supernova at 10 kpc, is nevertheless 20/kton total for  $\nu_e$  and  $\bar{\nu}_e$ , and 253/kton total for all other neutrino flavors [54]. This implies a total of  $\sim 76$   $\nu p$  proton-scattering events to be observed in Borexino. Similar considerations for KamLAND suggest that (with at least two operational low-energy neutrino detectors) it will be possible to make a reasonably good observation of the energy spectrum of  $\nu_\alpha$  and  $\bar{\nu}_\alpha$  ( $\alpha \neq e$ ) supernova neutrinos from a nearby stellar event.

The actual mix of neutrino flavors, and the energy spectra observed for each, will depend on the details of physical processes occurring in the supernova. These are not yet completely understood, and the study of neutrinos originating in a supernova would provide much important new data.